Basics of Mixer-Ejectors for Quiet Propulsion

JAMES BRIDGES[†], KHAIRUL ZAMAN[‡], BRIAN HEBERLING[§]

NASA Glenn Research Center, 21000 Brook Park Rd, Cleveland, OH 44135

A series of numerical and experimental studies were made to take a fresh look at how a mixer-ejector exhaust system might provide noise reduction for the landing and takeoff operation of a commercial supersonic vehicle. Historical understanding of aerodynamic and acoustic behaviors were updated and employed to design candidate nozzle systems. New CFD-based noise prediction tools, applied to conceptual designs, predicted noise reductions of 3-5EPNdB for a few percent thrust loss. Complementary experiments confirmed some key insights, established accuracy of thrust calculations, and corroborated general acoustic trends. Experiments, however, showed where the conventional acoustic understanding of mixer-ejectors is missing several complications to the acoustic theory, most critically an intrinsic unsteadiness in ejector flows. This unsteadiness often resulted in ejectors that were substantially louder than a nozzle without ejector, not quieter. The paper concludes with recommendations for future work in mixer-ejectors which will be required if their promise is to be fulfilled.

I. Introduction and Motivation

NASA is currently working to knock down environmental barriers to supersonic flight, airport noise being a key barrier. A series of studies made by NASA researchers and by industry partners have focused on aircraft capable of carrying 50-80 passengers at a cruise Mach number of 1.4-1.8. This class of vehicle was labeled an "N+2" generation vehicle, indicating that it probably wouldn't be the first generation of commercial supersonic aircraft, expected to be business jets, but would represent a second generation where commercial airlines could deploy such aircraft. In the studies, jet noise was identified as the key noise source during landing and takeoff operations. In the search for exhaust concepts that could produce significant noise reduction, the mixer-ejector nozzle was often proposed. However, this concept, while superficially attractive [1], is not found in common practice, and historically research programs that investigated its use did not produce a successful practical design. Given the improvement in computational tools and understanding of jet noise in general, it was decided to explore the concept and find general design guidance that would hopefully lead to successful designs, both acoustically and aerodynamically.

An ejector is a device that involves a shroud around a jet nozzle in which secondary or ambient fluid is entrained by the primary jet. The net mass flow rate at the exit of the ejector is increased and the corresponding velocity decreased relative to those of the primary jet alone. Turbulent mixing at the interface of the primary and secondary streams causes the entrainment and therefore the efficiency of the device depends on the mixing process which in turn depends on geometrical as well as flow parameters. Use of enhanced mixing devices such as vortex generators or lobed mixers at the primary nozzle lip can significantly enhance the entrainment process and the resultant pumping of secondary flow. Configurations involving such mixers have been typically referred to as 'mixer ejector nozzles'.

There have been numerous previous studies on ejectors as fluidic pumps and as a device for thrust augmentation. The vast literature on the subject may be appreciated from the fact that Ref. [2], published in 1967, cited 585 prior publications, dating as far back as 1919. Much of the earlier work focused on analysis of ejector performance. Thrust augmentation and its application in Vertical/Short Takeoff and Landing (V/STOL) aircraft was addressed in many papers, (e.g., [3,4,5] and several prior works cited in [2]). Later publications continued to address ejector flow and performance theoretically as well as experimentally, e.g., [6,7,8,9,10]. Other investigations addressed applications of the ejector and methods for improving its performance, e.g., [11,12,13,14]. The list of citations given herein is far from complete and an interested reader may look up the bibliographies of the listed ones for other past work.

[†] Acoustics Branch, MS 54-3; AIAA Associate Fellow

[‡] Inlets and Nozzles Branch, MS 5-1; AIAA Associate Fellow

[§] Inlets and Nozzles Branch, MS 5-1; AIAA Member

While the phenomenon of thrust augmentation by ejectors is desirable and in cases like V/STOL engines, where high lift is desired during takeoff and landing, thrust augmentation disappears in forward flight due to increased ram drag. Reference [8] finds that thrust augmentation decreases with increasing flight Mach number and becomes zero at a flight Mach number of about 0.7. On the other hand, the ejector principle has been used successfully in a variety of non-flight applications, especially mass-flow augmentation. For example, it has been utilized for powering the 'free-jet' co-flow in a large-scale jet noise measurement facility at NASA Glenn Research Center (GRC) [15].

Ejectors also hold significant potential for jet noise reduction. This aspect of ejectors has also been addressed in many previous studies over several decades, e.g., [16,17,18,19,20,21]. The noise reduction potential stems from the fact that jet noise roughly scales as the eighth power of the exhaust velocity. A decrease in exhaust velocity by using an ejector would thus yield significant reduction in jet noise. As an example, assume that the velocity is reduced to 70% of the primary jet velocity with an ejector shroud that has an exit diameter 1.464 times the primary nozzle diameter (assuming 50% entrainment and uniform flow at the ejector exit, to satisfy continuity). Then from the principle $I \sim U_j^8 D^2$ (where I is noise intensity, U_j the jet exhaust velocity and D the ejector exit diameter, and assuming fixed observer distance), about 9 dB reduction in I may be expected for noise produced external to the ejector. The benefit would increase rapidly with decreasing exhaust velocity.

For noise reduction, the ejector principle was adopted in the design of a supersonic aircraft considered in a past NASA/Industry program, the High Speed Civil Transport Program (HSCT), conducted during the 1990's. By using an ejector with lobed-mixers, parametric variations yielded exhaust velocities that were less than 60% of the primary jet velocity [22]. For example, with primary-to-ejector area ratio of 2.8, exhaust velocities were reduced from about 2400 ft/s to about 1400 ft/s. This yielded a reduction in noise intensities by about 15dB, as measured at various polar locations (and roughly following the simple scaling law discussed in the previous paragraph). The resultant noise, in effective perceived noise level (EPNL) metric, satisfied strict airport noise regulation standards [22]. (FAR36 stage III levels were satisfied with margin; an interested reader may look up [23] for the definitions of noise standards). Unfortunately, the HSCT program was canceled in late 1990's due to other NASA priorities.

More recent efforts at producing a low-noise nozzle using the principles of ejectors, many proprietary and unreported, have focused on engine cycles with lower specific thrust. Like the HSCT concept, these ejector designs featured actuated elements. Unlike the HSCT concept, they were based on round exhaust systems and did not incorporate acoustic lining in the ejector. Representative was the work done under NASA's Supersonics Project in the 2010's, communicated in Reference [24]. Each ejector design suffered from intrinsic resonances which could not be traced to a single element, cavity, or flow separation feature. The designs were made with a high degree of realism, the designers presuming they understood the principles of noise reduction, but their failure at achieving noise abatement demonstrated that more fundamental work was needed if a successful low-noise mixer-ejector was to be realized. The advent of desktop CFD and acoustic analogy predictions methods based on steady flow calculations, unavailable in previous generations of investigations, promised a better outcome. However, as will be shown, these insights are often overshadowed by intrinsically unsteady behavior, global resonances, that will require time-accurate prediction methods to fully resolve.

This paper covers the recent work of many researchers at NASA, some previously covered in References [25,26,27,28], but much of it new, and is intended to meld the insights gained into a coherent document. Several other variations on mixer-ejectors were studied, but not described here, as the focus of this paper is fundamentals of mixer-ejectors. These variants include thermal acoustic shields [29] and top-mounted propulsion for shielding [30].

The paper is broken into two parts, the first an overview of what is presumed known about aerodynamic and acoustic behavior of mixer-ejectors, starting with brief definitions. In the second part these understandings are illustrated and challenged by example studies, both numerical and experimental. The paper finishes with a summary and list of recommended future research topics.

II. Mixer-ejector parameter definitions

A mixer ejector exhaust system has two main components, a primary nozzle (also known as a forced mixer when enhanced mixing features are present), and an ejector. The primary nozzle emits air at pressure above ambient into the ejector. The ejector is a passive element with openings to ambient both upstream near the primary nozzle exit and downstream to allow both the primary air and air entrained within the ejector to leave. For propulsion systems, the primary nozzle is driven by the engine. Because of its geometric simplicity, this study primarily used an 8:1 rectangular primary nozzle with the ejector inlet confined to the broad side of the rectangle. Basic ejector design parameters are shown in the cross-section view of Figure 1. While the experimental part of the study was initiated with the 'one-sided' configuration as shown in this figure, the study also included more conventional geometry with ejector inlets

symmetrically on top and bottom. In the course of our study many of the parameters were varied, but in this report the focus will primarily be on the parameters found most important: ejector length and the height of the ejector exit, which sets the ejector-to-primary area ratio.

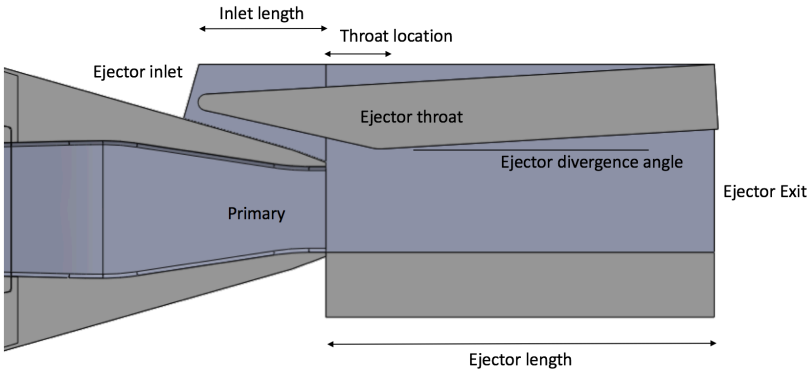

Figure 1. Basic mixer-ejector terminology

Because the amount of air entrained by the ejector is dependent on the mixing of primary and entrained air within the ejector, modification to the primary nozzle are often employed. For this reason the primary nozzle is also known as the mixer or forced mixer.

Mixers come in several flavors. In these studies mixers were classified as either lobed or chevron, although there is a continuum of designs that connect the two types of mixers, as illustrated in Figure 2. The one-sided ejector studies used chevrons exclusively (far right of Figure 2). A list of parameter nomenclature and representative values studied is given in *Appendix A. Nomenclature.*

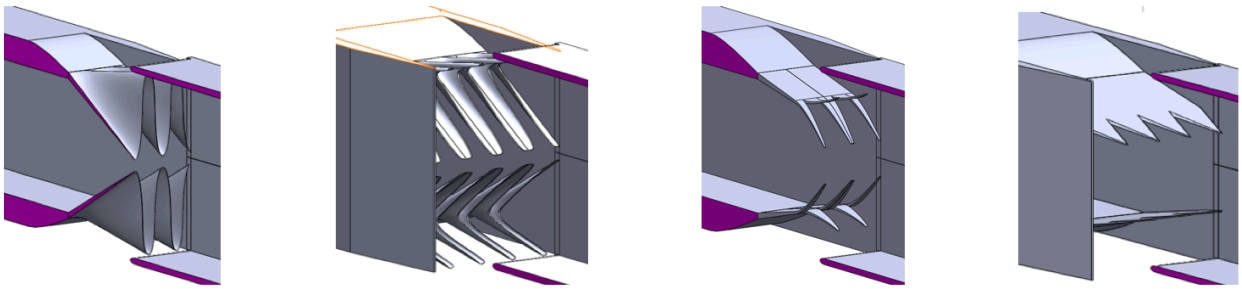

Figure 2. Range of mixer designs, from lobed to chevrons

III. How mixer-ejectors work—aerodynamics

A. Aerodynamic bookkeeping

Thrust is change in momentum over a control volume of a nozzle system. In simple nozzles, thrust is the stream force (momentum plus pressure differential) at the nozzle exit. For these simple nozzles, the pressure and friction forces on the outer surfaces are negligible. In practice, the nacelle forces must be considered, but may be considered part of the airframe for bookkeeping purposes. For mixer-ejectors, the process is more complicated. There are multiple flow streams and pressures on surfaces which play a large role in the thrust of an ejector. Figure 3 is a two-dimensional sketch of an ejector system used to illustrate two methods of computing thrust.

Direct method: See Figure 3a. The control volume is drawn on the outside of the nozzle, crossing ejector inlet and exit, but not including the primary stream. Since the outside of the solid is ambient pressure with minimal flow (grey lines), only bookkeep the momentum and pressure forces at flow openings (blue lines). This includes tracking the momentum and pressure forces on the ejector inlet. Assume friction and pressure forces on outside (grey lines) are zero, including base (or trailing edge) pressures around the exit. For all these assumptions to hold, pressures on the surfaces with grey lines must equal ambient, which is rarely completely true. This method is suitable for hand calculations and bulk properties.

Indirect method: See Figure 3b. Calculate the forces on the control volume excluding those of the openings (green lines), including primary stream (blue line). Forces include friction and pressure on nozzle. The net force (thrust) is

then the inlet stream force (blue line) less the body forces on the nozzle (green lines). This method is suitable for CFD, requiring accurate calculation of body forces, but more easily accommodating complex geometries.

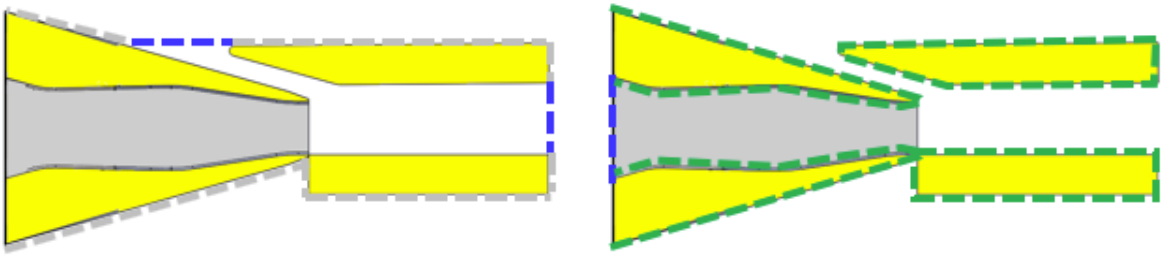

(a) *(b)*

Figure 3. Surfaces of integration for (a) direct method, and (b) indirect method.

B. Application to mixer-ejectors

Thrust of a mixer-ejector system can be considered in two parts: the efficiency of the mixer and of the ejector. The same considerations apply to the mixer as to any nozzle: pressure distribution, skin friction, and direction of efflux. Many mixers with high mixing efficiency lose thrust because they are redirecting the stream force away from the thrust axis. For the ejector, thrust is effectively lost/gained by pressures on ejector body; thrust is always lost by the friction forces on the ejector and by bringing low-momentum fluid across the control volume at the ejector inlet.

Besides the stream force common to all nozzles, only pressures on axially oriented surfaces contribute to axial thrust. (These surfaces must be within the control volume in calculations!) Entrained air produces vertical velocity past ejector inlet lip, decreasing pressure and 'pulling' the ejector forward. The bigger the surface, such as the bellmouth inlet on the ejector in Figure 4, the better the entrainment and the bigger the area for low pressure to increase thrust. In this fashion, the mass-augmenting ejector can produce thrust augmentation. However, with forward flight, the stagnation pressure of the flight stream on the inlet lip quickly overcomes the static pressure of the vertical velocity from entrainment, canceling the augmentation or yielding a net loss of thrust. Figure 5 shows how the pressure distribution on the bellmouth changes from favorable (low pressure on the forward-facing surface), to adverse (high pressure) as the nozzle is flown.

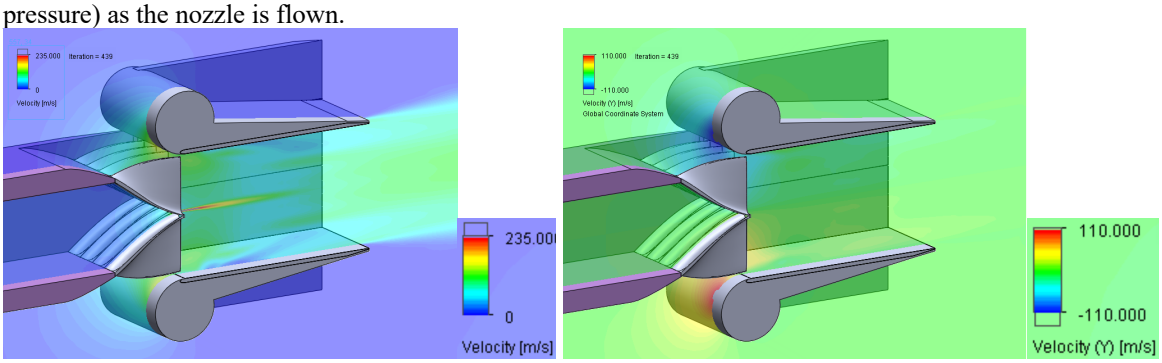

(a) *(b)*

Figure 4. Bell-mouth ejector with lobed mixer, showing (a) total velocity and (b) vertical velocity fields.

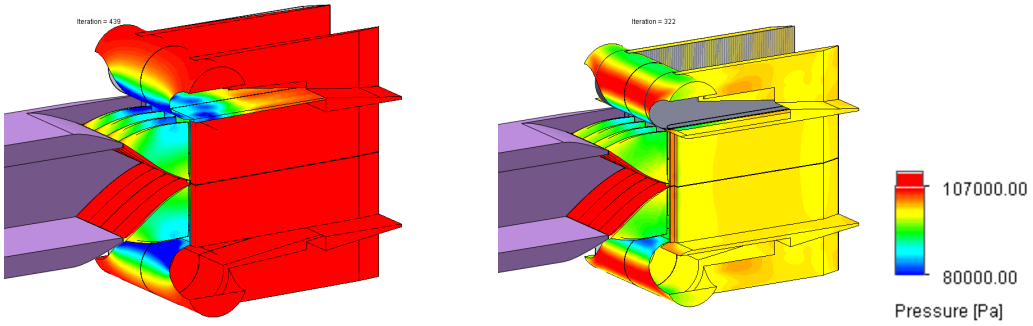

(a) *(b)*

Figure 5. Static pressure on surface of bell-mouth ejector with (a) no flight, (b) flight at M=0.3.

Points to remember about aero performance of ejectors:

- Ejectors augment thrust by creating low pressures from entrained air past upstream-oriented lip surfaces.
- Bringing on low-speed air into the nozzle control volume reduces thrust.
- Having more surface (ejector body) normal to thrust axis reduces thrust with increased flight speed.
- The mixer used to promote the entrainment of the low- and high-speed air can have high aerodynamic losses as a result of misdirected momentum and unrecovered pressure drops.

The aerodynamic performance can be optimized by mixer design, by minimizing the ejector friction losses, and by avoiding internal flow separations. Internal separations must be strictly avoided to have good thrust and avoid resonances. To reduce thrust loss in flight, the projected area of the ejector should be minimum. This is the fundamental dilemma of mixer-ejectors for thrust enhancement—the greater the thrust enhancement created at static conditions the greater the thrust penalty as flight speed increases.

C. Validation of CFD thrust predictions

To validate calculations of thrust and thrust bookkeeping methods, the thrust of a one-sided ejector was measured at ASE FluiDyne Aerotest Laboratory ("ASE"). Both a standard ASME nozzle of the same size and four configurations of the ejector were tested without forward flight and compared with computations. Details are contained in Reference [31].

SolidWorks® Flow Simulation (SWFS) was the flow solver used primarily in these ejector studies. SWFS does not use a body fitted mesh generated from the part surface, but rather a cut-cell Cartesian mesh generated globally and dynamically refined during the solution process. SWFS solves the Navier-Stokes equations supplemented by fluid state equations defining the nature of the fluid, and by empirical dependencies of fluid density, viscosity, and thermal conductivity on temperature. For turbulent flows, the Favre-averaged Navier-Stokes equations are utilized and closed using the modified k-ε turbulence model with damping functions. In later work, the NASA Langley Navier-Stokes solver 'FUN3D', which uses body-fitted unstructured grids, was used. Similar results were obtained, although the details varied between the two solvers, possibly reflecting the difficulty in finding a steady solution in what can be an intrinsically unsteady flow.

The results of the ASE tests are given in Figure 6, along with the predictions obtained using SWFS CFD calculations. The calculations were made using resolution and convergence strategies typical of exploratory work, i.e. not the highest resolution possible. Both direct and indirect methods were used to compute the thrust coefficient, *Cfg*.

The SWFS estimates of thrust for the ASME nozzle were nominally within the error bar of the experiments, especially the direct method (Figure 6a). For the one-sided ejector, four configurations were tested and predicted (Figure 6b). The red data represent the baseline case without chevrons, with an ejector area ratio *EjAR*=1.35. *EjAR* is defined as the ratio of ejector exit area divided by mixer exit area. The other three configurations are with chevrons on the mixer: the blue for same *EjAR* as the baseline, green for a larger *EjAR* = 1.57, and black for an ejector with divergent flaps. For the baseline ASME nozzle as well as the one-sided ejector calculations, the indirect method gave a higher estimate for *Cfg*, commonly by around 0.5%. Increased grid resolution around the nozzle body reduced this discrepancy at the cost of increased calculation times. General trends in *Cfg* for changes in ejector parameters and flows were captured within the 0.5% uncertainty. This exercise gave confidence in the thrust trends captured in explorations of different configurations and in insights, such as those above, given by the CFD.

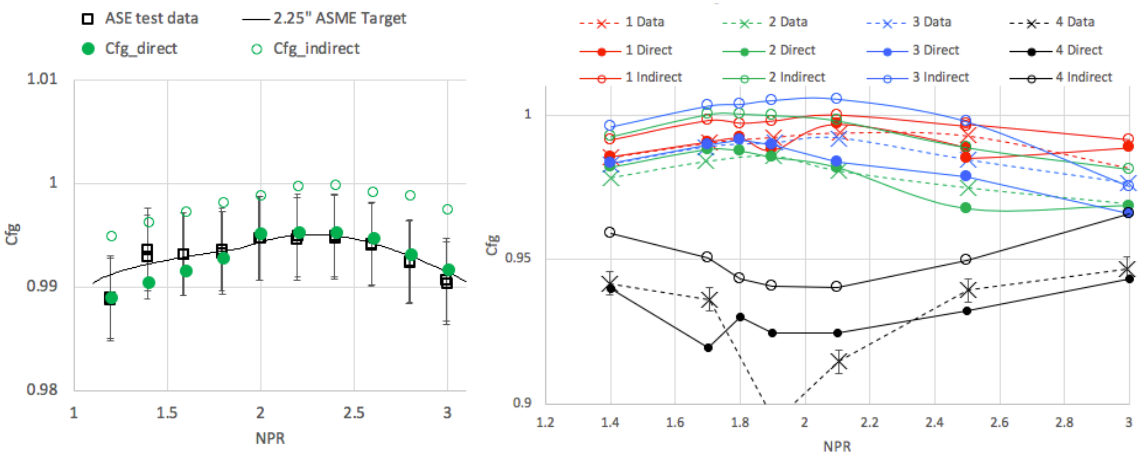

(a) *(b)*

Figure 6. Thrust coefficients *Cfg* measured and computed using direct and indirect methods using SWFS for (a) ASME nozzle, and (b) four one-sided ejector configurations over sweep of nozzle pressure ratios (*NPR*).

IV. How mixer-ejectors work—acoustics

The conventional picture of how ejectors reduce noise is that by inducing a co-flow around the primary stream the jet external to the ejector has reduced velocity, hence reducing the jet noise. If a forced mixer is employed, the external jet velocity outside the ejector is reduced even further. However, this is oversimplified. Two main factors can produce adverse effects:

- While high frequency noise of the initial shear layer is being shielded by the ejector, the enhanced mixing process makes additional noise. The additional noise will not be entirely absorbed/shielded.
- The flow within the ejector may rapidly switch between several quasi-steady states, producing a resonance and strong tones.

In addition, the following may also contribute to additional noise:

- A new shear layer is formed at the ejector exit, producing new high frequency sources which may be more energetic than expected due to excitation by the residual turbulence of the internal mixer.
- The turbulence from the mixer will produce some trailing edge noise as it passes over the ejector exit. Historically this has been termed ‘excess noise’[32].

Key to understanding how to lower Effective Perceived Noise Level (EPNL), the metric used to judge aircraft noise, is an understanding how frequency and directivity impact the annoyance, the weighted sound pressure level which integrates to become EPNL.

The acoustic sources of a mixer-ejector nozzle system, operating in a steady (not resonant) manner, are the usual ones found in jet exhaust systems, small-scale and large-scale mixing noise, broadband shock noise, and trailing edge dipole noise. The broadband shock noise will arise once primary flow conditions become supersonic, and may be mostly internal to the ejector. The trailing edge dipole noise comes from the internally generated turbulence of the mixer passing over the trailing edge of the ejector. The small-scale mixing noise will arise from the shear layer of the internal mixer and the fresh shear layer of the ejector trailing edge. The shielding of the former is one of two main concepts in low-noise ejectors. The large-scale mixing noise, where convection velocities of large-scale vortical structures couple efficiently with the far-field pressure, is mainly external to the ejector, and is impacted by the reduction in jet velocity due to the enhanced mixing of the internal mixer. This is the other main concept in how ejectors reduce noise. In this report, the expectation is that engine cycles of interest will have nozzle pressure ratios at or slightly above sonic, where some broadband shock noise may arise in the initial portion of the primary mixer flow, but will be mostly located within the ejector. It will be the small-scale mixing noise, from the shear layer of the internal mixer and possibly from the ejector trailing edge, that will produce the high frequency noise at broadside angles that impact human annoyance. The large-scale mixing noise will contribute low-frequency noise to the aft angles, impacting the duration of the noise in the EPNL calculation. Simultaneously minimizing these two sources would be the secret to a low-noise mixer-ejector.

To illustrate these ideas, we will use predictions of far-field spectral directivity and source distributions from the combination of RANS CFD (SWFS) and a simple acoustic analogy code *mSrc* [33]. This code captures much of the conventional understanding of mixing noise sources in conventional jets. We will apply this to a rectangular nozzle, scaled to 2000 square inch exit area, operating unheated at NPR=2. The EPNL is essentially the integrand of the annoyance, itself a transformed version of the spectral directivity of noise. In the transformation, the spectra are weighted to account for the frequency response of human hearing (which peaks around 2000Hz), and with polar angle transformed to time given the flight path of the aircraft. In the carpet plot of annoyance plotted in Figure 7a we see two peaks, one at 10*log*(*Freq*)=26 (400Hz) and another at 10*log*(*Freq*)=33 (2000Hz), both at broadside angles to the jet axis. Tracking backwards to the source distributions at the key frequencies and polar angles, we see where the sources are produced (Figure 7b).

When an ejector is applied to the rectangular nozzle (Figure 8) there is a small reduction in both the high and low frequency peaks (Figure 8a). Looking at the source distributions that contribute to these peaks, we see that a substantial portion of the high frequency source region in the bare nozzle (Figure 7b) is covered by the ejector. We also see a substantial reduction in size of the low-frequency source region compared to the bare nozzle.

Now, if the rectangular nozzle is substituted by a lobed mixer, the effect on the bare lobed configuration (no ejector; Figure 9) is to greatly increase the high frequency peak in annoyance, but reduce the low frequency peak substantially. As will be made clear later in the paper, the amount of increase at high frequencies will be key to the acoustic success of the mixer-ejector. The source region of the high frequency noise is high in amplitude and very close to the mixer. The low frequency source region is smaller than that of the bare rectangular nozzle, in keeping with the reduced jet velocity downstream. Now when an ejector is applied to the lobed mixer (Figure 10 the high frequency peak in annoyance is reduced and the low frequency peak is reduced as well. Looking at the source distributions (Figure 10b), the reduction in high frequencies seems largely due to shielding by the ejector. The reduction in the low-frequency peak is due to the reduced downstream velocity by the combination of the mixer and ejector. That is, relative to the rectangular mixer, the enhanced mixing of the lobed mixer greatly reduces the velocity downstream of the ejector. Relative to the bare lobed mixer, the ejector forces ambient air into the mixing process due to the lowered static pressure within the ejector, again resulting in lower jet velocity downstream of the ejector. The result is an exhaust system with a predicted 5.5EPNdB reduction from the bare rectangular nozzle in Figure 7.

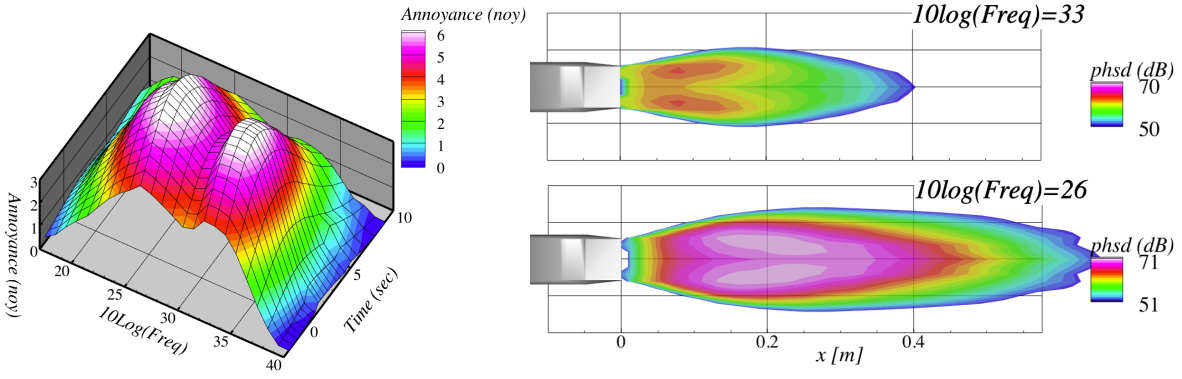

(a) (b)

Figure 7. Rectangular mixer without ejector: (a) Annoyance and (b) source regions for peak annoyance. 81.4EPNdB.

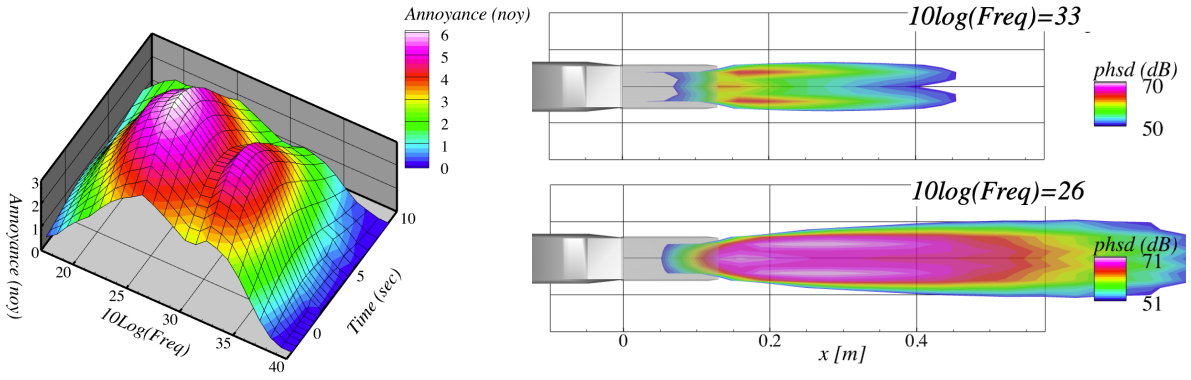

(a) (b)

Figure 8. Rectangular mixer with ejector: (a) Annoyance and (b) source regions for peak annoyance. 79.6EPNdB

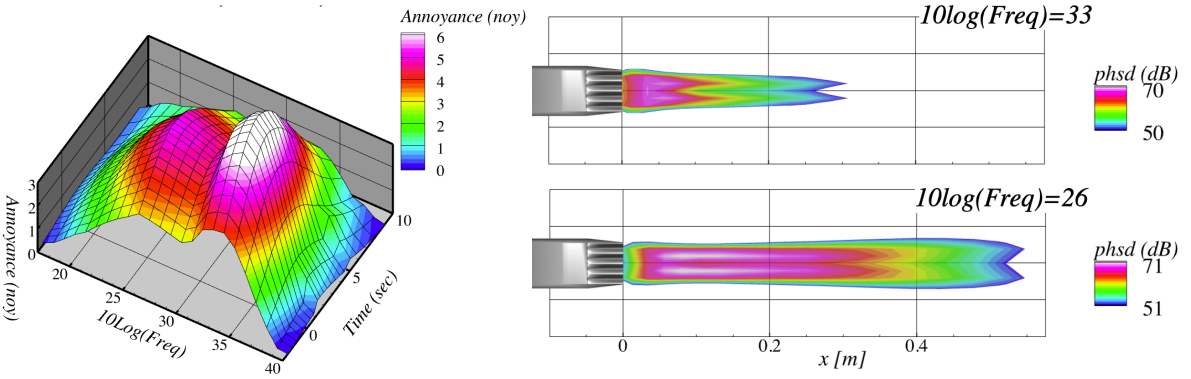

(a) (b)

Figure 9. Lobed mixer without ejector: (a) Annoyance and (b) source regions for peak annoyance. 80.3EPNdB.

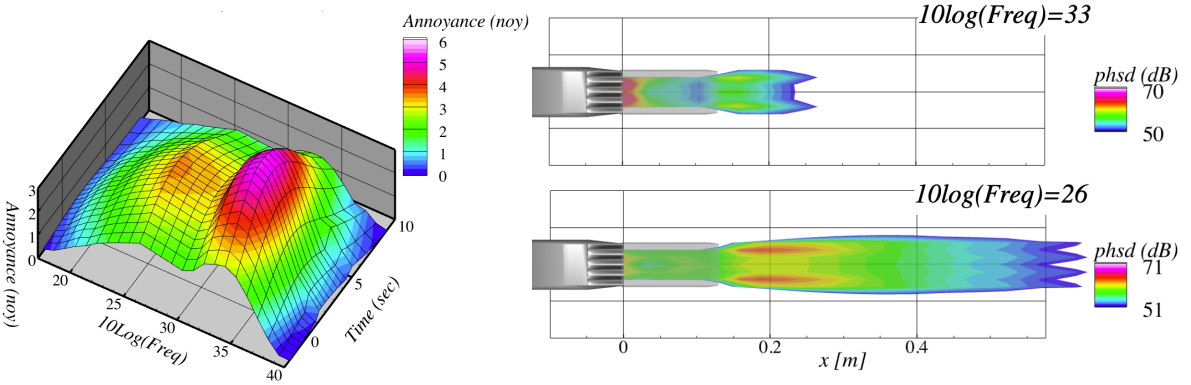

(a) (b)

Figure 10. Lobed mixer with ejector: (a) Annoyance and (b) source regions for peak annoyance. 75.9EPNdB.

In an ideal world, the ejector absorbs all the mixing noise made within it, and the mixer is 100% effective in mixing the entrained flow. No sources exist within the ejector and the flow at the exit is uniform (in this example having pumped in 31% ambient relative to the primary flow, the most of any mixer tried here). In that case, the annoyance and noise source maps would be as in Figure 11. This ideal exhaust system produces 10.5EPNdB less than the bare rectangular nozzle. Note that there are still sources in the shear layer of the rectangular jet emanating from the ejector, but they are greatly reduced in strength because of the reduced velocity in the plume. It is idealistic approximations

such as this that have made a mixer-ejector appealing to many who seek large reductions in jet noise. There are many reasons why this is unrealistic and several will be covered in this paper.

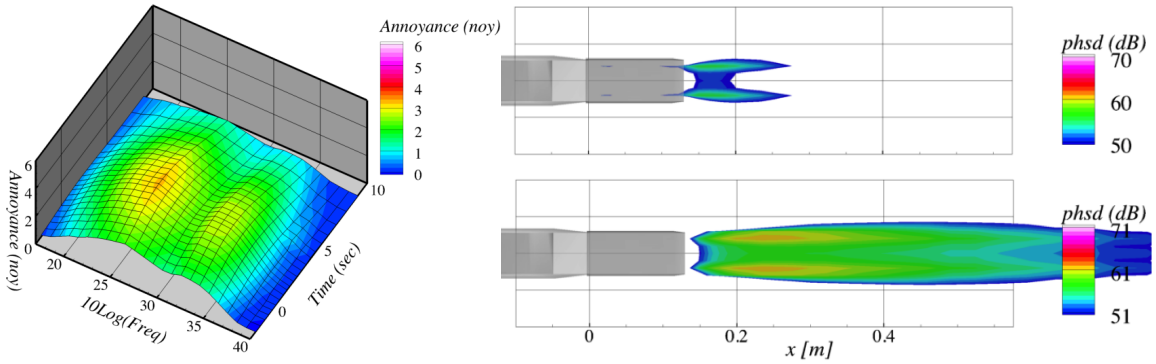

(a) (b)

Figure 11. Ideal mixer-ejector: (a) Annoyance and (b) source regions for peak annoyance. 70.8EPNdB.

We explored many mixer-ejector combinations numerically using the SWFS+*mSrc* prediction method shown above. There were many mixer-ejector combinations where the enhanced mixing did not result in as much low frequency reduction, where the enhanced mixing made more noise than could be contained in the ejector, or where the shear layer produced at the exit of the ejector was a significant contributor to the high frequency peak. There were several shortcomings to the acoustic prediction method: First, there was no model for the trailing edge dipole produced as turbulence generated by the mixer inside the ejector passed over the ejector lip. Second, the acoustic prediction method uses a very simplified shielding model to predict how sound produced inside the ejector was propagated out to the observers. Third, the analysis method, being limited to steady flows by its use of RANS for the flow calculation, could not predict the inherent unsteadiness of mixer-ejector flows. This phenomenon creates resonances as was discovered in subsequent experiments, and which is a much bigger acoustic problem than those listed above. This will be covered in Section VI below.

V. Importance of mixer-ejector parameters on aero performance

Numerical studies of thrust were conducted on two families of mixer-ejectors, both on rectangular primary nozzles with 8:1 aspect ratio detailed in Reference [9]. The first study was of a one-sided ejector, while the second study used a two-sided mixer-ejector. Experimentally, flow diagnostics were made on several of the configurations in NASA Glenn's CW17 jet rig to check the computations. These studies, experimental and numerical are described in the next section, focusing first on single-sided ejectors and then on double-sided ejectors.

A. One-sided ejector studies--experiments

Figure 12 shows the geometry of the one-sided ejector system in which the ejector length, divergence angle, flap leading edge, intake gap height *G*, ejector exit height *H*, number of mixing chevrons, length of mixing chevrons, and upper surface microvortex generators could be varied. Because there are a multitude of length scales for non-dimensionalization, all dimensions in the figure are given in inches. Note that the length of the ejector was varied by adding extensions at the downstream end (not shown). The photos in Figure 13 show the mixer-ejector mounted in NASA Glenn's CW17 jet rig, and show a closeup of the chevron strip used to enhance mixing of the rectangular primary nozzle.

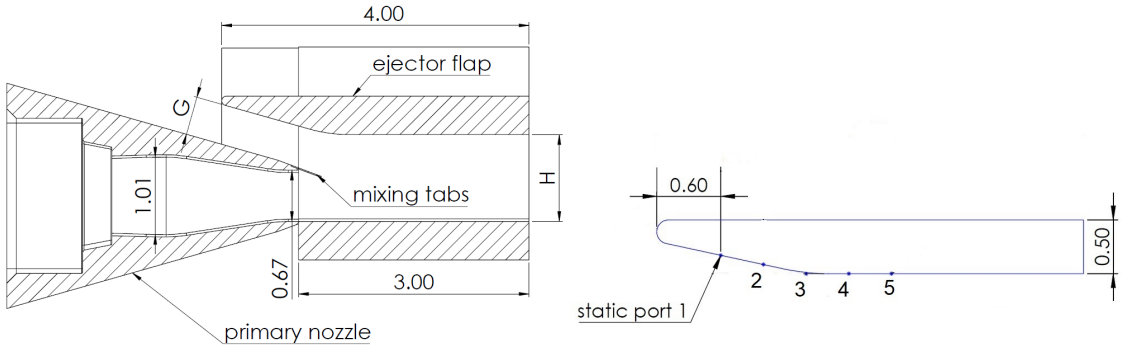

(a) *(b)*

Figure 12. One-sided ejector geometry (a) cross-section of mixer-ejector, (b) location of static pressure ports in ejector.

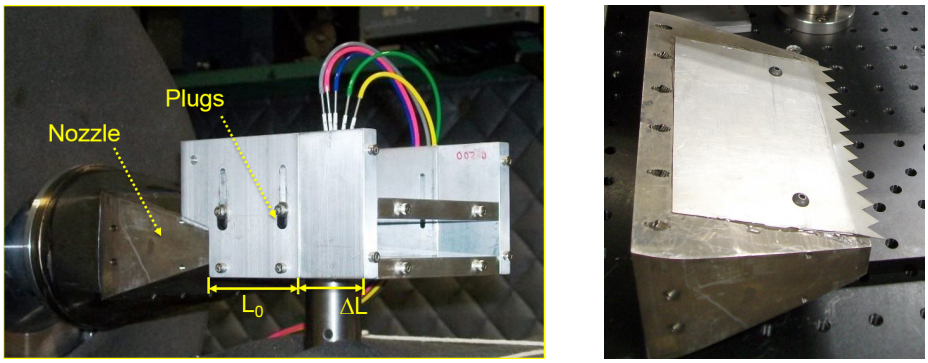

(a) *(b)*

Figure 13. Photo of one-sided mixer-ejector (a) mounted in CW17, (b) chevron strip for enhanced mixing.

Integrated pitot probe surveys of the ejector exit plane showed how much pumping the various ejector configurations gave for both the rectangular and chevron mixers. Figure 14 shows this measurement versus ejector area ratio and versus ejector length and divergence angle. Without chevrons there was very little pumping, a point made clear by comparison to the modest chevron mixer for various ejector heights (Figure 14a). The contour plots of the Mach number at the ejector exit (Figure 15) show that the ejector with rectangular mixer left large portions of the ejector exit with essentially no flow. By contrast, the chevrons mixed the flow across the ejector opening until the largest ejector area. At this ejector area ratio the pumping of the chevron mixer-ejector decreased, quantified by a reduction in the mass flow at the ejector exit.

Divergence angle of the ejector wall acts somewhat like ejector area for the chevron mixer, as seen in (Figure 14b). Increasing the exit area while leaving the ejector throat (inlet gap G) fixed increases the divergence angle of the ejector, which produces more entrained mass flow until a point (here between 4° and 6°) where the ejector flow separates, causing less mass flow to be entrained. Ejector length, plotted here as the ratio of ejector length L divided by baseline mixer height h, was not found to be a significant factor in the amount of entrainment without divergence.

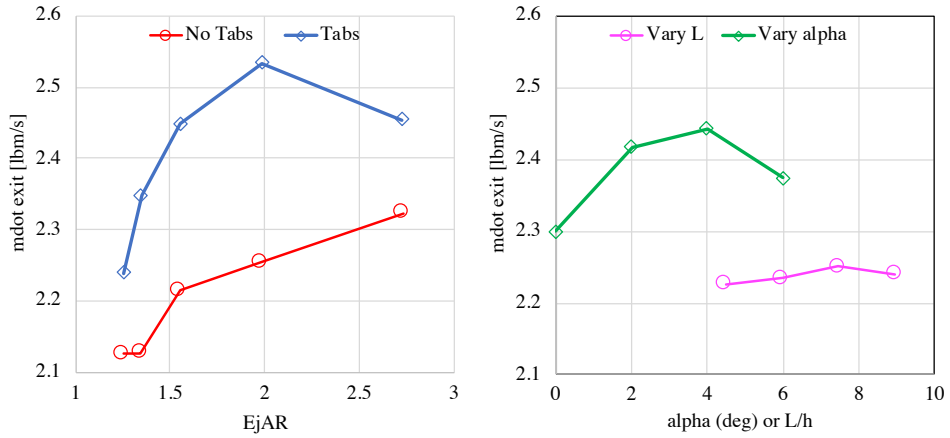

(a) *(b)*

Figure 14. Mass flow rate at exit of ejector (a) as function of ejector area ratio *EjAR*, with and without chevrons, (b) as function of ejector divergence angle α and ejector length *L/h* for chevron mixer, with same inlet gap *G* as $\alpha = 0°$, *EjAR*=2.75. M_j =0.9.

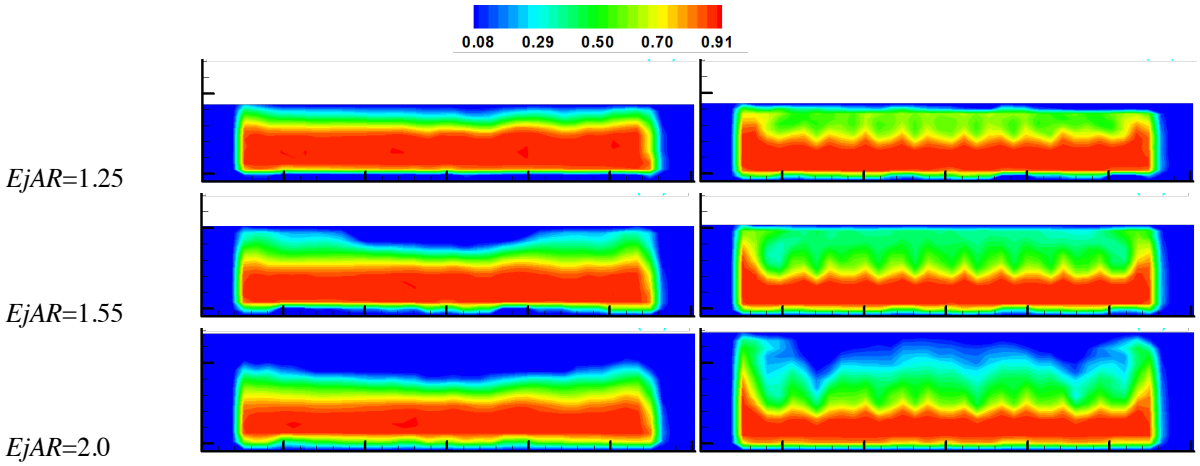

(a) *(b)*

Figure 15. Mach number contours 0.04inch downstream of ejector exit for different *EjAR* as indicated; M_j=0.9. (a) rectangular mixer, (b) chevron mixer.

The role of the chevrons was further reinforced by looking at the static pressures within the ejector (Figure 16). With the rectangular primary nozzle, all locations within the ejector have similar static pressures for a given primary Mach number, and this pressure only decreases slightly with increased primary Mach number. With the chevron mixer, the static pressure is very low on the forward-facing side of the ejector inlet as air is sucked into the ejector by the pumping action of the chevron mixer. The static pressures along the main body of the ejector are similar to that of the rectangular mixer. The inlet static pressures drop very quickly with increased primary Mach number, showing the ejector to be most effective at high speeds. Details of the data in Figure 14Figure 16 are contained in Reference [26].

These trends were confirmed in numerical studies presented next, and the ability of the CFD to replicate the Mach contours measured at the ejector exit gave confidence in the extensive numerical studies, described next.

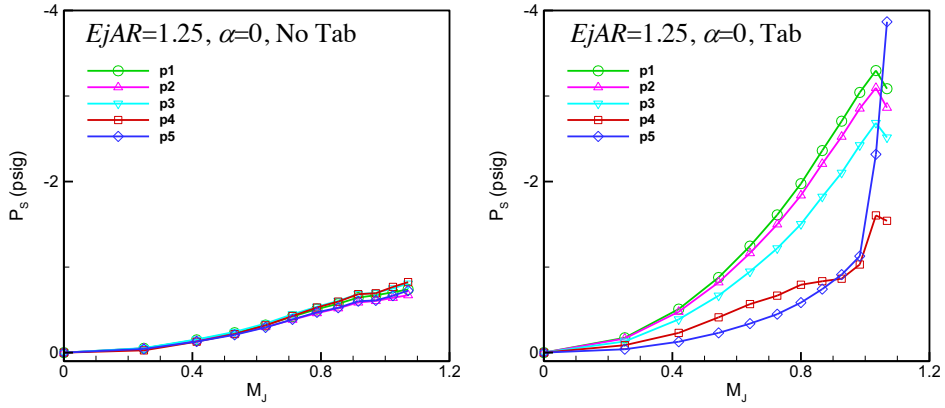

(a) *(b)*

Figure 16. Static pressure versus M_j. Each graph has data from the five ports. (a) rectangular mixer, (b) chevron mixer.

B. One-sided ejector studies--simulations

The primary objective of the numerical simulations of the one-sided ejector was to validate the CFD against initial measurements made in the CW17 facility. The mixer-ejector configurations have two features that are commonly difficult to get correct with RANS: turbulent mixing and in some cases boundary layer separation. The comparisons with the data presented above demonstrate the degree to which the simulations should be trusted.

In the experiments, the flow at the exit of the ejector box was surveyed and integrated to obtain a measure of the entrainment for various ejector geometries with and without chevrons on the primary nozzle (Figure 14). These flows were simulated using SWFS, and the mass flow at the exit plane was computed for a direct comparison with the experiments (Figure 17). Comparing Figures, the mass entrainment was consistently underpredicted by 5-10%, while the experimental data had an uncertainty/repeatability of ~5%. Arguably, the separation that causes the decrease in ejector exit mass flow at highest α (Figure 14b) was not captured in the simulations. This would be in keeping with the common observation that RANS codes do not predict separation well.

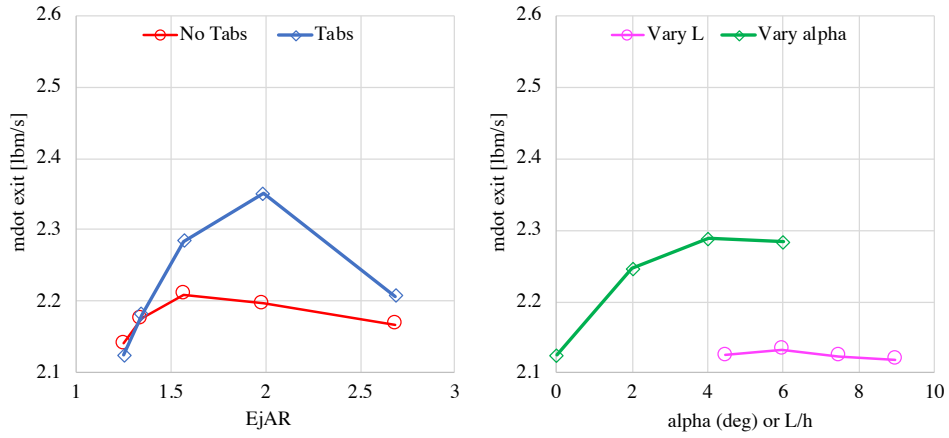

(a) *(b)*

Figure 17. Same as Figure 14 except results are from SWFS.

The Mach number contours at the ejector exit can give some indication of how well the mixing process was simulated. Comparing Figure 15 (experiment) and Figure 18 (simulation) shows that relative agreement in the mass flow was not a fluke. The primary nozzle without chevrons has a flow at the ejector exit which is nearly independent of the ejector area The chevron primary produces high speed flow that fills the ejector at *EjAR*=1.35 and 1.57, but leaves a layer of low-speed air with the same thickness when the ejector is very large (*EjAR*=2.0). And even though the CFD obviously has enforced symmetry which the experiment does not, the velocity contours are well reproduced, including the details of the sidewall flow.

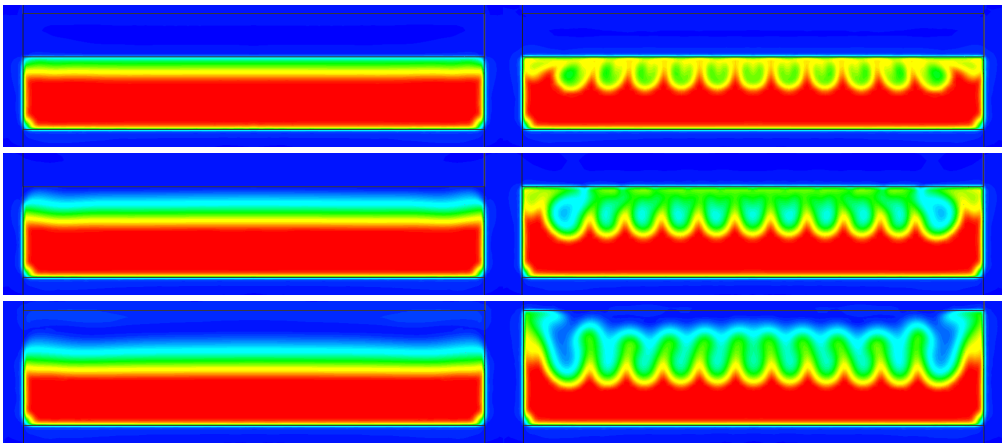

Figure 18. Same as Figure 15, except results are from SWFS.

In summary, trends in ejector fluid mechanics are well represented by the SWFS computations and all interesting features were reproduced by the computations. As shown above in Section III.C thrust calculations were just outside experimental uncertainty.

As chevrons are a geometrically simple mixing enhancement device, and enhanced mixing is a key aspect of mixer-ejectors, the simulations were next used to explore how simple changes in chevron geometry impact the ejector aero performance. Ejector geometry was fixed with $EjAR$=2 and ejector length L/h=4.5. The two parameters that were varied were the number of chevrons and length of the chevrons. The set of chevrons always spanned the primary nozzle with each individual chevron being of equal width and the ends of the chevron strip finishing with half-chevrons. The number of full chevrons was varied in increments of two from 5 to 11 chevrons and the length was varied from 0.17 to 0.67 inches (primary nozzle height h is 0.67 inches). The chevrons have an inclination of 20° to the jet axis. The flow condition was M_j=0.9, unheated. There were no experiments to validate these predictions.

Two aero parameters were monitored in this study, thrust coefficient Cfg and the pumping ratio m_{exit}/m_{prim} - 1. Note that the pumping ratio is similar to the ejector exit mass flow measured in experiments above, but normalized to account for the changes in primary flow due to differences in blockage by the different chevrons and difference in static pressure generated within the ejector. Figure 19 presents the aero parameters as a function of chevron length for the four chevron counts. Cfg increased with number of chevrons until the chevron count reached 9. Interestingly, this was true for all chevron lengths, so the driving parameter must be the spacing of the vortices, not the aspect ratio of the chevrons. For each chevron count a length of roughly 0.334 inch produced the best Cfg. Similarly, the pumping ratio also found that the number of chevrons was not significant for chevron counts of 7 and higher. Increasing chevron length increased the pumping ratio over the range of lengths studied here. Taken together, for any chevron count the pumping ratio continues to increase with increased chevron length while Cfg maximizes at a modest chevron length. This implies that the losses caused by the longer chevrons was not offset by the decreased static pressure on the leading edge of the ejector caused by the increased pumping. While this optimum chevron design might be different for different ejector designs, this exemplifies the finding that aero performance of mixer-ejectors is not a monotonic design space. More pumping does not equal more thrust; mixer design is critical.

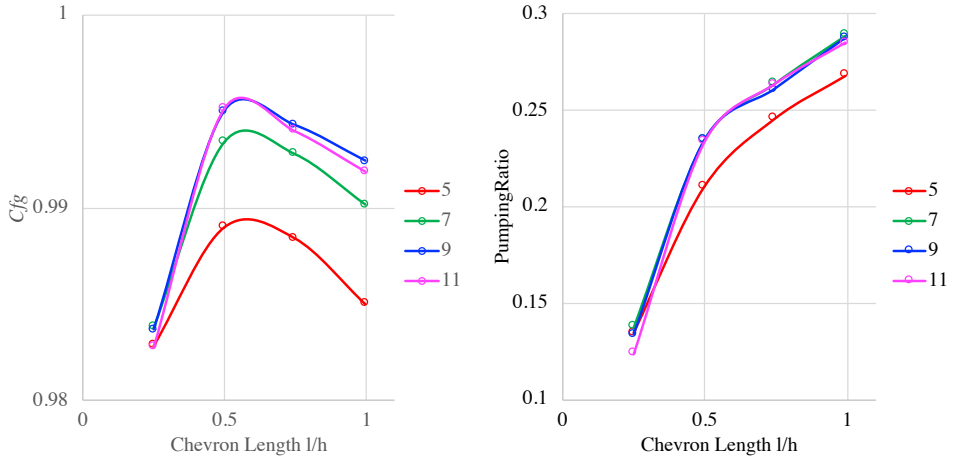

(a) *(b)*

Figure 19. Aero performance of one-sided ejector with varying number of chevrons, chevron length.

C. Two-sided ejector studies

A further study was conducted using the same basic rectangular geometry as above, but having symmetric ejector inlets. The rectangular nozzle was heavily modified to explore the impact of multiple chevron and lobe-style mixer designs. The effective mixer area was held roughly constant for all the mixers, as checked by the mass discharge without an ejector. The ejector box was maintained with no divergence and a fixed width matching the wide dimension of the 8:1 mixer, but the box was varied in height (ejector area) and length.

1. Mixer geometry studies

Many variations on lobed mixers and on chevron mixers were conceived and studied, and the findings can only be summarized here. In general, mixer designs encounter three issues for thrust while trying to enhance mixing: skin friction from extra flow surface, adverse pressures from separations, and misdirected flow. For lobed mixers, the important parameter for thrust seem to be how well the flow is turned back to the axial direction. If the lobes end with the flow having significant transverse velocity, mixing is enhanced but thrust is reduced. Similarly, cutting back the sidewall of the lobes improves mixing and reduces skin friction, but penalizes thrust from the misdirection of the flow. This is demonstrated for a series of lobed nozzles (Figure 20) that differ in the degree the flow is turned back to the axial direction before the mixer exit. Names given to the mixers are purely in order of their creation, not any parameter value.

In modern lobed mixer design the sidewalls of the mixer are often cutback, reducing skin friction and weight, and increasing vorticity generation. Figure 21 shows two of the mixer designs considered that had such cut-back sidewalls on the lobes of the mixer. Note that if the sidewalls are cut back enough, the lobed mixer begins to look like a chevron mixer with alternating chevrons!

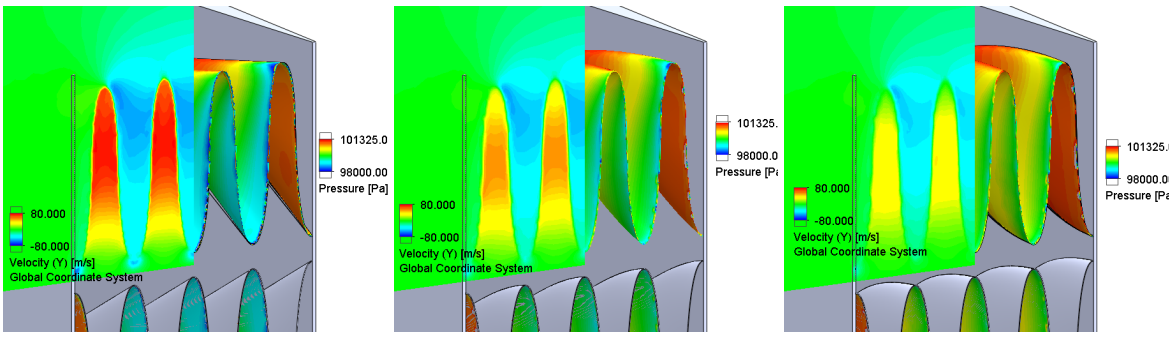

Lobe1, *Cfg*= 0.983 Lobe4 *Cfg* = 0.991 Lobe5, *Cfg* = 0.994

Figure 20. Demonstration of non-axial flow and adverse pressures reducing thrust. Fully lobed mixers with varying degrees of lobe exit angle. Vertical velocity components at exit plane of mixers, pressure on mixer.

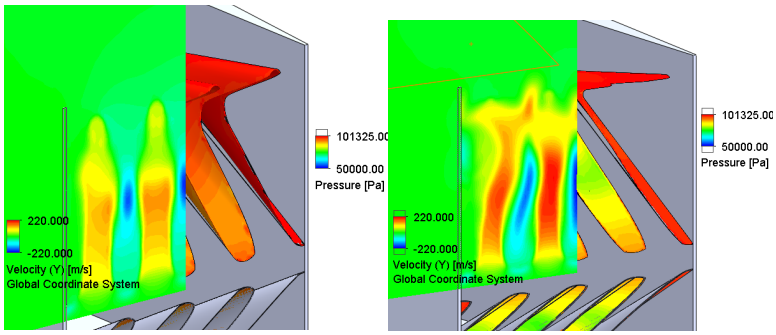

Lobe2, *Cfg*= 0.936 Lobe3 *Cfg* = 0.853

Figure 21. Demonstration of non-axial flow and adverse pressures reducing thrust. Cutback lobed mixers with varying degrees of cutback. Vertical velocity components at exit plane of mixers, pressure on mixer.

For chevrons, losses from the induced low pressure on the downstream side of the chevron hurt thrust, as it will for lobes with highly scalloped sidewalls. These are in addition to losses from nonaxial flow. Figure 22 shows the vertical velocity at the exit plane of the chevron mixer and surface pressures below ambient which contribute to thrust loss. The more aggressive mixers reduce the downstream jet velocity better than the nonaggressive ones, but the thrust cost is high.

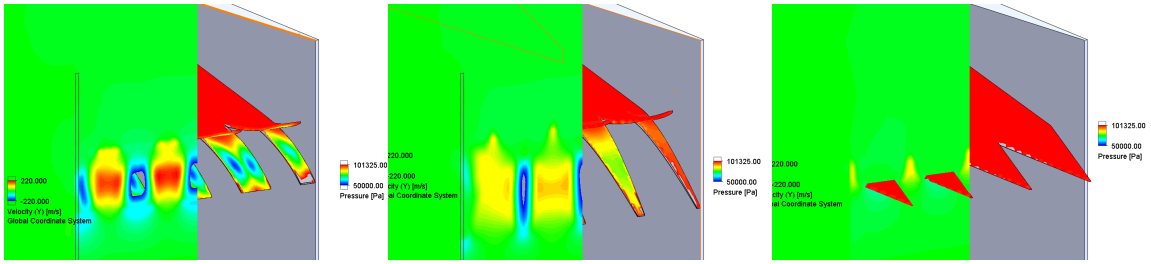

Chev2, *Cfg*= 0.923 Chev3, *Cfg* = 0.952 Chev1, *Cfg* = 0.998

Figure 22.. Demonstration of non-axial flow and adverse pressures reducing thrust. Chevron mixers with varying degrees of blockage. Vertical velocity components at exit plane of mixers, pressure on mixer.

2. Ejector geometry studies

Ejector length: Three ejector lengths were run on five of the mixers, including the rectangular mixer. The mixers included high-mixing and high-performing lobed and chevron mixers. The ejector area ratio was 2.2, the smallest of the ejector areas studied. As seen in Figure 23, the *Cfg* generally decreased with increasing ejector length, just as was observed in the one-sided ejector study. The pumping ratio (m_{exit}/m_{prim} - 1), a measure of entrainment, increased significantly for all mixers as the ejector length became greater than its height, but a further doubling did not bring additional entrainment.

Ejector area ratio: Three ejector area ratios *EjAR* were run with three lobed mixers and the rectangular mixer. The ejector length was 1.2 times its height, the middle length studied in Figure 23. Figure 24 shows the thrust coefficient and pumping for these cases. In general, increasing ejector area ratio had a small, detrimental effect on *Cfg*, and mixers with higher mixing (identifiable by their relatively poor performance) did lose more thrust with increased area ratio. The pumping did increase with increased ejector area, except for the rectangular mixer, where there was very little mixing even at the smallest ejector area. The strange downturn in pumping for Lobe5 mixer at the largest ejector area seems to be because the primary flow could no longer drive the entire ejector flow downstream and there was reverse flow at the ejector exit. This is a warning that if a mixer with mostly axial exit flow is used, it must span the entire height of the ejector.

Pumping vs Cfg: Although it is contained in these figures, the overall relationship between entrainment and thrust needs to be brought out explicitly. Figure 25 plots pumping vs *Cfg* for all the mixer-ejectors studied. From here one can see that there is no overall relationship as each is independently dependent upon the geometric details of the mixer and of the ejector. *Cfg* is primarily governed by the performance of the mixer and secondarily by the velocity of the entrained flow past the upstream lip of the ejector and the forward-projected area of that lip. These characteristics are interdependent, but not uniquely so. In other words, there is no unique relationship between *Cfg* and pumping.

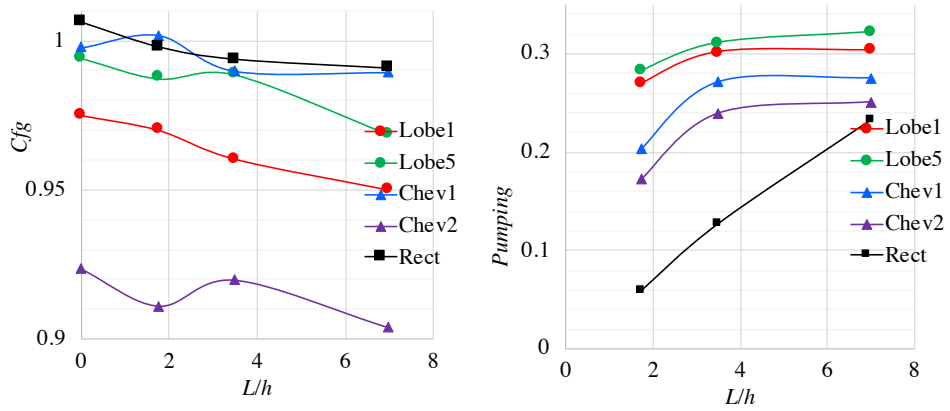

Figure 23. Effect of ejector length on thrust and pumping ratio for five mixers.

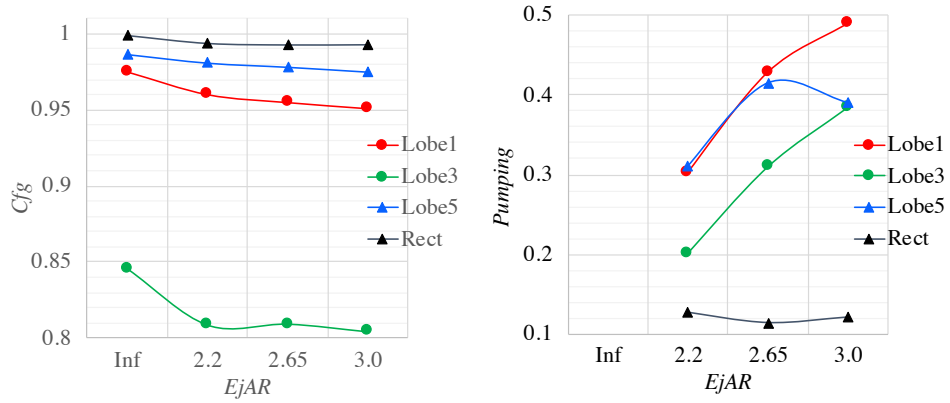

Figure 24. Effect of ejector area ratio ($EjAR=A_{exit}/A_{prim}$) on thrust and pumping for lobed mixers

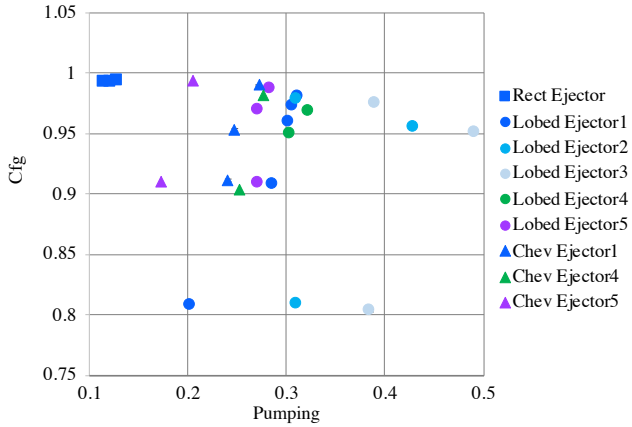

Figure 25. Relationship between thrust and pumping for mixer-ejectors studied for thrust performance.

Flight effect studies: Because the ejector being used here had a minimal thickness and leading edge area, it does not produce thrust enhancement, but it does not suffer much degradation in thrust when the nozzle is in flight. Figure 26 shows how the *Cfg* and pumping change with ambient flight speed for the Lobe1 mixer (Figure 20) and ejector with $L/H = 2.2$, $EjAR = 1.2$. The thrust loss and pumping increase are nearly linear with flight speed. The thrust coefficient drops from 0.97 to 0.935 as the flight speed increases from stationary to $Mach = 0.3$. Contrast this result with the bellmouth inlet on the high-*EjAR* configuration in Figure 4, which dropped from 1.16 to 0.56 over the same flight speeds. (The pumping ratio went from 2.63 to 2.95.) Forward motion kills ejector performance as suction on forward surfaces is quickly turned to ram drag when the aircraft begins to move.

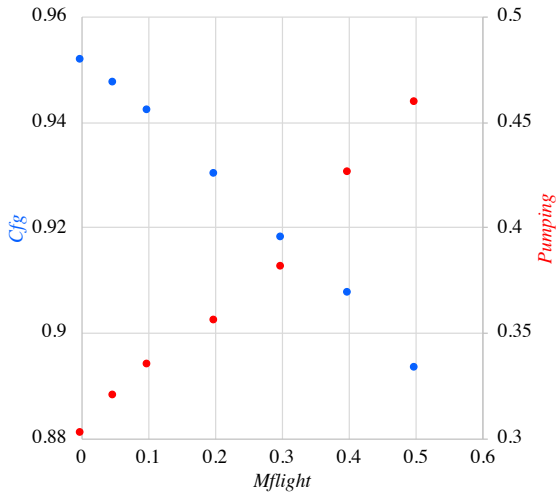

Figure 26. Thrust and pumping variation with flight, for thin ejector lip.

VI. Importance of mixer-ejector parameters on acoustic performance

The experimental facilities of the small test cell CW17 used to investigate flow parameters of the single-sided ejector are not conducive to accurate noise measurements as the test cell is not anechoic. In addition, a great many explorations of acoustic performance were carried out numerically with acoustic prediction tools that used many assumptions.

Tests were made on the one-sided ejector described in Section VI A above, and on two-sided ejectors based on the same nozzle system to confirm general trends for noise in mixer-ejectors. The tests were carried out at the NASA Aero-Acoustics Propulsion Laboratory on the Small Hot Jet Acoustic Rig (SHJAR). The SHJAR is a single-stream jet rig [34], and in this set of tests only acoustic measurements were made; no aero data was obtained in this test.

A. One-sided ejector studies--experiments

Possibly the most valuable thing learned in the noise explorations of one-sided ejectors in the non-anechoic CW17 facility was to beware of flow resonances in mixer-ejector systems. While this has been anecdotally observed in tests over the decades, this was very prevalent in the 2-D mixer-ejector with a rectangular mixer. Figure 27a shows the noise spectra measured on the SHJAR for the same ejector and primary flow conditions, but with and without the chevrons on the primary nozzle. Without the chevrons, the jet howls, producing not only very strong tones but also a broadband noise level amplified by over 10dB. Comparisons of the sound from the two primary nozzles, without the ejector, are given in Figure 27b. The peak levels are within 2dB of each other.

The other observations made from Figure 27b that generically held true are that adding mixing enhancement lowers the low frequency peak noise level and increase the high frequency end of the spectrum. It is also generally true that putting the primary nozzle within an ejector reduces the high frequency noise produced by the mixing enhancement devices. Usually one sees a further reduction in the low frequency peak, but the one-sided ejector does not promote as much mixing of the primary flow as if the ejector were open on all sides of the primary nozzle. This is a significant observation—for an ejector to work for noise, the jet plume must be allowed to mix strongly from all sides. This is also why placing an exhaust system directly onto a top aero surface in a top-mounted installation will not be acoustically successful. The jet plume peak velocity must be reduced for the downstream source to be significantly reduced. For this, we turn to the two-sided ejector geometry.

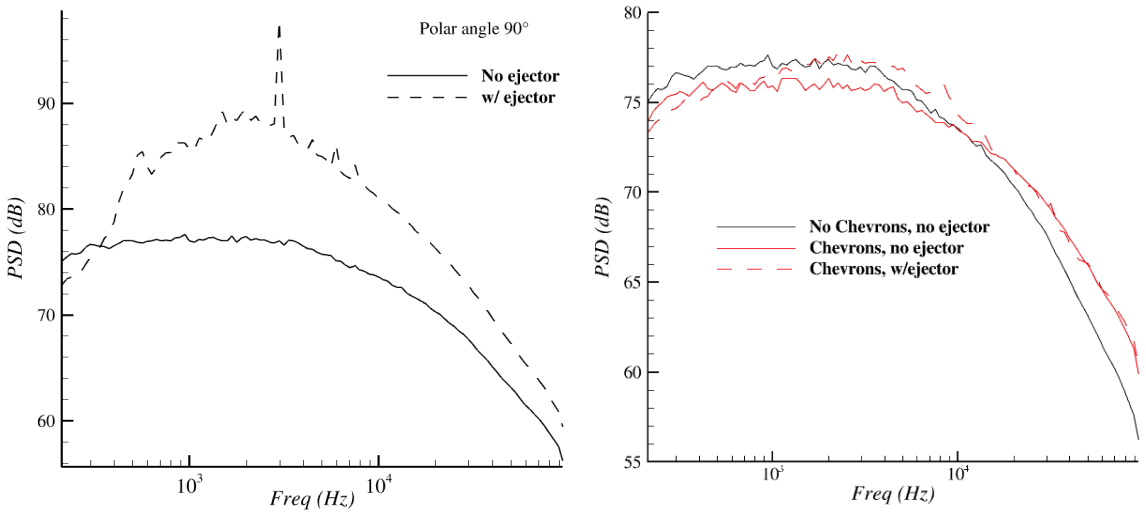

Figure 27. Measured noise spectra for one-sided ejector at 90° to jet axis. (a) Comparison of rectangular and chevron primary nozzles in half-ejector, *L*/*h*=4.5, *EjAR*=1.35. (b) Comparison of bare rectangular nozzle, bare nozzle with chevrons, chevron nozzle with same half-ejector.

B. Two-sided ejector studies—simulations and experiments

Many rectangular mixers and ejectors were explored numerically using SWFS and *mSrc* in the fashion shown above in Section IV. The trends followed what was discussed there, with changes in ejector length and ejector area ratio making only a small difference on the noise when an unforced mixer (rectangular nozzle) was used. Configurations with a forced mixer were predicted to have much greater acoustic impacts, with several of the mixer-ejector designs promising large reductions in EPNL.

A matrix of design parameters was chosen to validate experimentally. These parameters were ejector mode, mixer type, ejector height (area ratio), and ejector length, with values given in Table 1. Configurations were named using a four-character sequence of these codes in the right-to-left order given in the Table. Of the 75 possible configurations, 42 were simulated, and 30 of those 42 configurations were tested. The results discussed below represent the findings of these predictions and experiments.

Depictions of the three mixers, without ejector and with various ejector modes and heights, are shown in Figure 28. The chevrons used on the chevron mixer were placed on the lip of the rectangular nozzle in an alternating skip pattern (Figure 28b), best described as starting with 11 chevrons on each side and removing every other chevron in an alternating pattern across the nozzle. Each chevron was 0.68 inches long, had a length-to-width ratio of 3:2, and made an angle of 20° to the flow axis. The lobe mixer had 8 pairs of lobes 1.87 inches peak-to-peak, with widths adjusted to give the same exit area as the rectangular nozzle. A minimal set of subsonic-to-low-supersonic flow conditions were tested, and in the results reported below the primary flow was unheated, with a nozzle pressure ratio of 1.856, which produces a jet of roughly acoustic Mach number 0.9 in the bare nozzle.

Table 1. Mixer-ejector parameters for experimental validation tests.

Mode			Mixer			Ejector Height EjH			Ejector Length EjL	
Code	Description		Code	Description		Code	[inch]		Code	[inch]
N	No ejector		N	8:1 rectangular		A	1.09		3	3
D	Double-sided ejector		T	8:1 rectangular, with alternating chevrons		B	1.54		5	5
S	Shielding only		L	8:1 lobed mixer		C	1.94		8	8
						D	2.46		A	0
						N	∞			

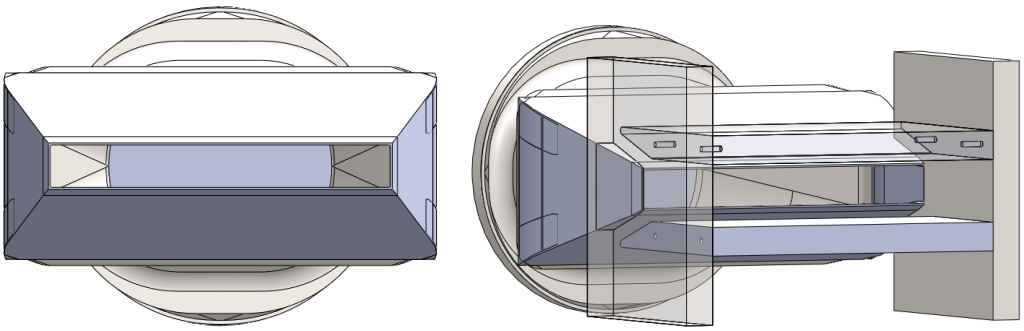

(a) Rectangular mixer, left: NNNA; right: DNA3

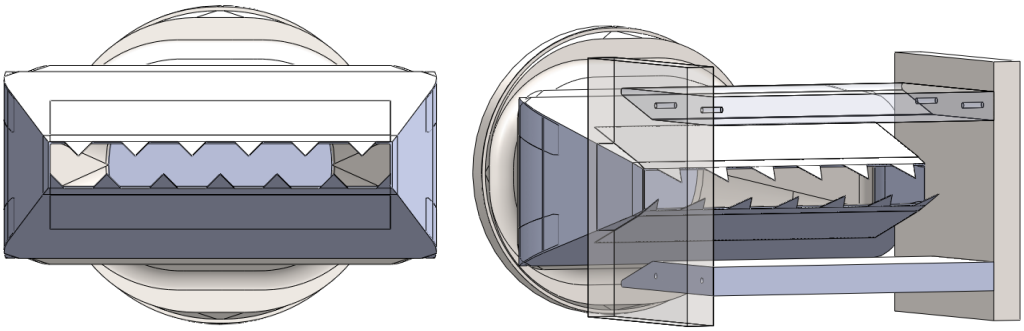

(b) Chevron mixer, left: NTNA; right: DTD3

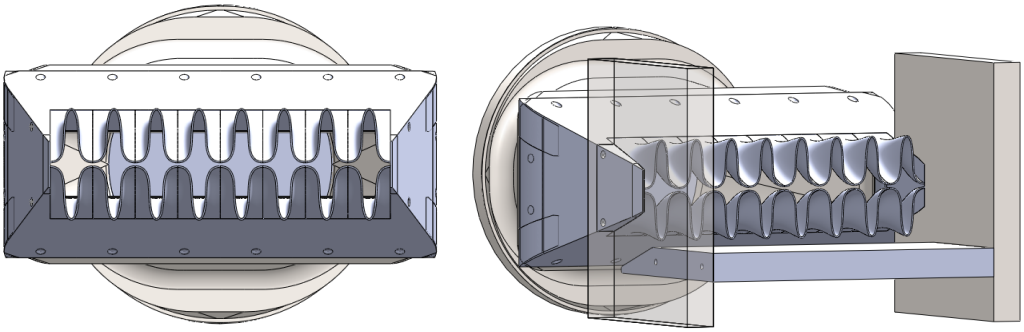

(c) Lobe mixer, left: NLNA; right: SLC3

Figure 28. Representative configurations used in study, featuring the three mixers, shown without ejectors and with different ejector heights, including in shielding-only mode.

The spectra at polar angle 90° is shown in the presentation of far-field acoustic results below, being representative of the change in the overall noise. The plots are of noise power spectral density in model scale, given by the frequency of the bottom axis. The spectra have been transformed to a 1-foot distance assuming spherical spreading from the mixer exit with the atmospheric attenuation lost during propagation to the microphones added back to the spectra. Tying these results back to the discussion of how mixer-ejectors are expected to impact EPNL (Section IV above), the full-scale frequency is shown on the top axis of each plot; the range of full-scale frequencies shown is 50Hz – 10kHz, matching the range included in EPNL calculations. The model-scale nozzle has exit area 3.24 inch^2 while the full-scale nozzle has exit area 2000 inch^2, intended for a tri-jet commercial supersonic aircraft.

A key aspect of the design of mixer-ejectors is the forced mixer. Acoustically, the shift of acoustic energy from low to high frequency by the mixer is the basis for the change in total noise. As shown in Figure 29a, the chevrons and lobes were predicted to shift energy from low to high frequencies; however, as shown in Figure 29b, more energy was added than expected. Moreover, when scaled to fullscale the energy lies within the strong annoyance range of 2-3kHz, which negatively impacts EPNL relative to the baseline bare rectangular nozzle. This puts forced mixers at a disadvantage compared to the baseline of an unforced rectangular nozzle, requiring significant shielding of this noise by the ejector if the total noise is to be reduced. As will be shown, the ejectors did not overcome this handicap.

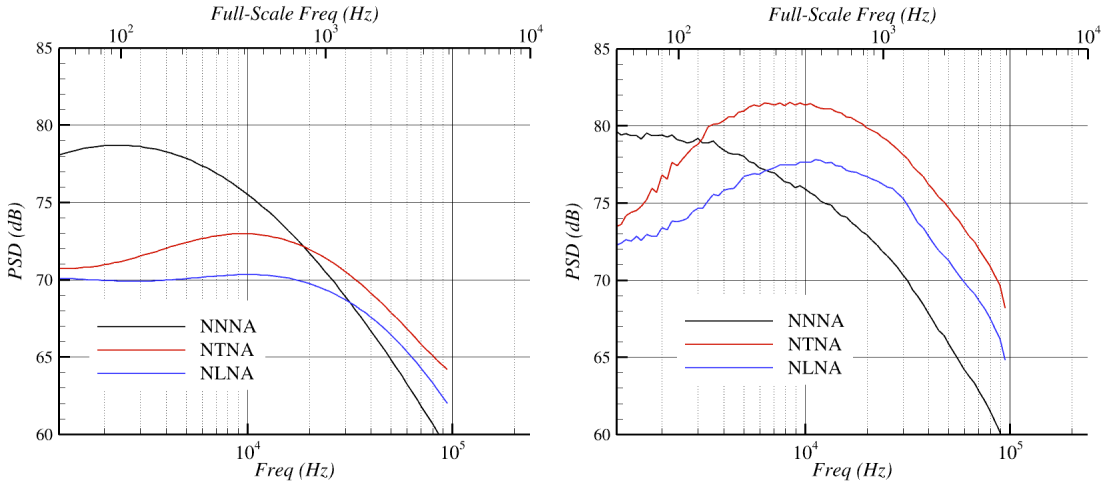

Figure 29. Noise spectra of mixers without ejectors. (a) predicted, (b) measured.

When ejectors are added to the mixers, they are expected to shield a significant portion of the high frequency noise generated near the mixer exit. When applied to a rectangular mixer, the effects were expected to be relatively small, as shown in Figure 30a. However, as shown in Figure 30b, these configurations were plagued with resonances which overshadowed any acoustic shielding of noise internal to the ejector. This was true of all configurations using the rectangular mixer. Forced mixers, discussed next, often suppressed the resonances; however, there were many forced mixer configurations that showed resonance of less intensity, often at lower speeds than shown here.

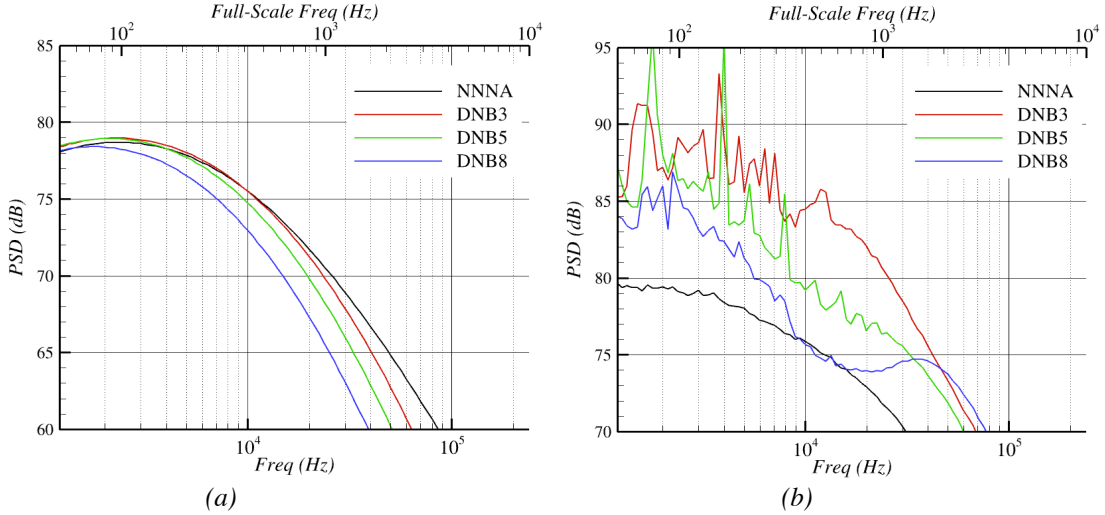

Figure 30. Noise spectra of rectangular mixer N with ejector height B and varying lengths, including no ejector. (a) predicted, (b) measured.

When an ejector was applied to a forced mixer, there were indeed reductions in noise, but the impact was not as simple shielding. Figure 31a shows the spectra for the bare chevron mixer without ejector and with three different lengths of ejector of moderate height (B). Comparing the noise of each ejector with the bare mixer, the ejector was expected to reduce the mid-and high-frequency noise of the bare mixer by 5-8dB. In Figure 31b, the relative levels are shown to be consistent with predictions near the spectral peak of the bare chevron mixer, but at high frequencies the ejector produced more noise than it shielded. Clearly, the impact of the ejector is not just to simply block the same acoustic sources that were present without the ejector.

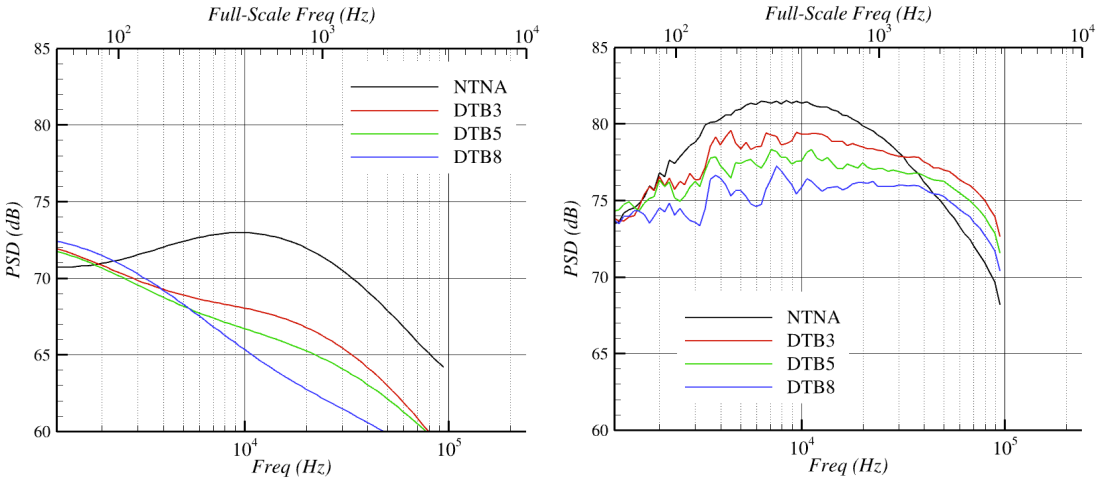

Figure 31. Noise spectra of chevron mixer T with ejector height B and varying lengths, including no ejector. (a) predicted, (b) measured.

Figure 32 shows the predicted changes in turbulent kinetic energy produced by the addition of an ejector on the chevron mixer. The bare chevron mixer produces a very expanded plume, which is strongly modified when the ejector is applied to the mixer. For example, a region of high turbulence a few nozzle heights downstream of the bare mixer (top shear layer in the plot) does not develop within the ejector as the high-speed plume hits the ejector wall before the turbulent region develops. Instead the high-speed flow along the wall produces a new shear layer at the exit of the ejector, albeit with weaker intensity, that is unshielded and has different turbulence lengthscales. While the figure only shows a slice through a very three-dimensional plume (the asymmetry of the chevron pattern causing the upward angle on the centerline shown), it illustrates the extent to which applying an ejector to a mixer is not just an acoustic modification to the source field of the bare mixer.

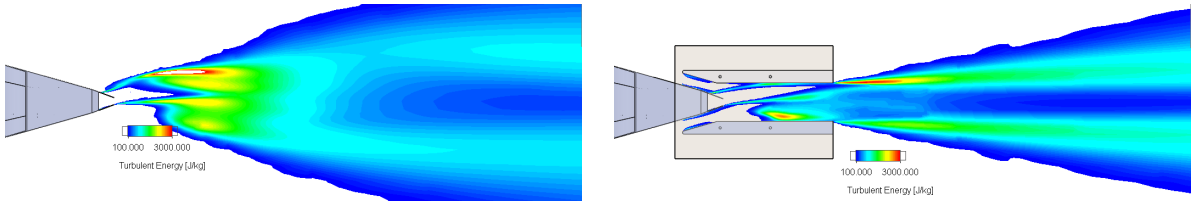

Figure 32. Predicted turbulent kinetic energy along center plane of chevron mixer (a) without ejector and (b) with ejector.

The acoustic impact of changing ejector area ratio, here produced by changing the height of the ejector leaving the ejector walls parallel, was not predicted to be simple. Due to the modifications to the flow by the presence of the ejector it is no surprise that changing the capture area of the ejector would produce a change in the complex internal flow and hence the noise. Predictions based on these changes in the turbulence found differences of over 5dB in the spectra as shown in Figure 33a. The changes were not monotonic with increasing ejector height, alluding to a more complex change in the acoustic sources associated with the changes in turbulence. In the experiments (Figure 33b), the variations with ejector height did produce non-monotonic behavior with ejector height, just not the ones predicted. Clearly, with the largest height (DTD5) there is unsteady flow separation producing to low frequency noise. This also provides a cautionary note that even ejectors with strong forced mixers can have flow unsteadiness and resonances that cannot be predicted by steady CFD methods. As mentioned above, the rectangular mixer without chevrons produced resonance at all ejector configurations. In the case of the chevron mixer in Figure 33b, the impact of ejector area ratio was overshadowed by the noise from the unsteady behavior.

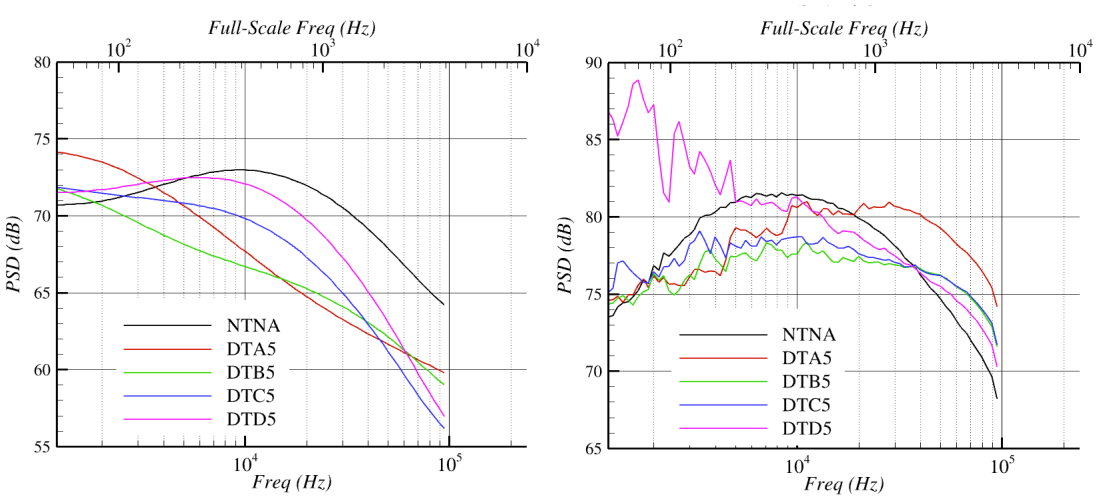

Figure 33. Noise spectra of chevron mixer T with ejector length 5 and varying heights, including no ejector. (a) predicted, (b) measured.

A third mode of configurations were also explored, noted in Table 1 as Shielding. The naïve point of these configurations was to isolate the aerodynamic impact of the ejector, namely the reduced static pressure at the mixer exit induced by the ejector, from the acoustic impact, shielding of acoustic sources near the nozzle. By removing one wall of the ejector, in this case the inlet wall opposite the far-field observer, there would be no reduced static pressure, and hence no increased entrainment.

As shown in Figure 34a, adding length to a shield, e.g. an open-sided ejector, increasingly blocks high frequency noise generated near the chevron mixer from reaching the far-field observer in the model. This simplistic idea was largely borne out by the test findings, Figure 34b. The differences between the unshielded chevron mixer and the various lengths of shield are very similar in the predictions and experimental results. One important feature not shown in these plots is the trailing edge dipole that arises from jet-surface interactions; the trailing edge dipole occurs at very low frequencies, below 1kHz in model scale, and hence off the left of the plots. This noise source does not impact the EPNL calculation but would be important in aircraft design, for structural reasons if nothing else. Also of note is when a shield was applied to the rectangular nozzle, the configuration produced resonance in experiments, but of a different spectral character than the ejector on the rectangular nozzle.

Compared to an equivalent ejector, the shields did not have as much mid-frequency noise, either because the noise was redirected away from the observer instead of being bounced around inside the ejector and back to the observer, or because the ejector did not develop resonance.

Note that over the entire frequency range of interest in full-scale EPNL calculations, the shielding configurations showed reduction over the bare chevron mixer. However, due to the miss in predicting the spectra of the chevron forced mixer, predictions of EPNL benefits compared to an unforced bare nozzle were wrong. Still, judging by the relative similarity in the spacing between curves in Figure 34a and Figure 34b, the application of a simple shielding model in the predictions was found to be relatively accurate in the absence of resonance. With the reductions produced by shielding, total reductions in EPNL of a few dB were found. This was significant, although nowhere near as dramatic as the 10EPNdB reductions that were predicted. Here the main error in the prediction is the modeling of the mixing noise from the chevrons, which is a much more efficient process in converting TKE to noise than a round jet.

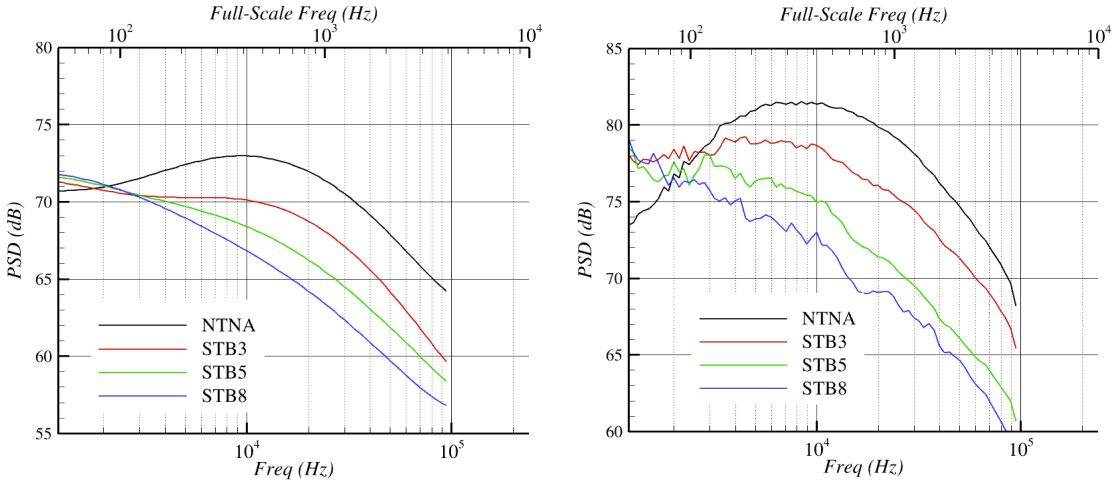

Figure 34. Noise spectra of chevron mixer T bare and with shield at height B, varying shield length. (a) predicted, (b) measured.

VII. Recommendations

Possible research activities to push the Technology Readiness Level of mixer-ejectors for low noise LTO aircraft include:

- ***Demonstrate LES on mixer-ejector.*** Based on difficulties discovered for jet-surface interaction, accurately calculating propagation/reflection of noise within the ejector will be difficult.
- ***Apply LES and URANS on CW17 resonance cases to confirm ability to detect phenomenon.*** Previous mixer-ejector tests have found global resonances to be a common problem. Prediction methods must be available to avoid designs with this flaw. Previous studies [35] of other nozzle with flow resonances have found that RANS does not alert the designer of the problem, URANS in unable to predict the resonance, and only LES was able to predict the large unsteadiness.
- ***Explore propulsion concepts using an actuated shield for under-aircraft installations***. If top-mounted propulsion is not viable for aerodynamic reasons, an actuated shield, deployed during landing and take-off operations, can provide significant noise reduction with less risk of resonance and less thrust loss than an ejector.
- ***Explore liners applicable to installation surfaces and ejector interiors.*** The predictions made here use a very simple assumption about how the ejector shields noise, when in fact more internal noise will propagate out if not attenuated by a liner. Models for surface attenuation and experimental validation must be developed.
- ***Develop aero/acoustic optimization of mixers using adjoint methods.*** Use of RANS-based adjoint methods to maximize thrust is currently being pursued; adding targets of TKE and/or noise sources is a stretch goal.

VIII.Summary

The concept of a mixer-ejector exhaust system has existed in technical literature for over a century, originally used to augment air moving systems. As applied to aircraft, they have been studied as thrust augmenters in applications where forward motion was not an issue, and in previous research programs for commercial supersonic vehicles, mixer-ejector nozzle systems were studied as a low-noise concept. The basic aero understanding is based on analytical models that have not been very thoroughly vetted, and the basic acoustic understanding is even more primitive. In the intervening 20 years since the last exploration of mixer-ejectors there has been a revolution in aero and acoustic prediction tools to better understand the potential of this type of exhaust system for efficient quiet propulsion. A wide-ranging set of studies were undertaken to revisit the problem of mixer-ejectors with the objective of obtaining insight into their aero and acoustic behaviors, and potential low-noise propulsion solutions.

Exploratory experiments using a very simple mixer-ejector geometry showed the importance of enhanced mixing devices on the primary nozzle. They documented the entrainment characteristics for variations in ejector length, exit area, and internal divergence. The basic data and insight obtained in these experiments were used to validate CFD tools that were in turn used to explore other mixer-ejector geometries. As a further validation of the computational methods used in the study, four configurations of the one-sided ejector were tested at a high-fidelity thrust stand (ASE FluiDyne Aerotest Laboratory) and the computational tools found to produce results only slightly outside the uncertainty of the test measurements.

The numerical studies of aero performance looked at the impact of basic ejector geometry and the effect of the mixer design, studying mixers that ranged from fully-lobed, to cutback lobed, to chevrons, and to apply these in the cases of one-sided and two-sided ejectors. The aero performance of the mixer-ejector, at least in the realm of propulsive exhaust systems, is dominated by that of the mixer, with ejector parameters having much less of an effect. For a given mixer, increases in entrainment by increasing the size of the ejector decreased the thrust. The ejector design does have a significant impact on aero performance when flight is considered; ejector designs with significant frontal area have a strong sensitivity to flight, quickly changing from beneficial to harmful with ambient flight speed. Ejector designs with little sensitivity to flight do not augment thrust.

Acoustically, the traditional view that ejectors reduce jet noise by lowering downstream jet velocity and shielding high frequencies was generally borne out. However, this is an incomplete view, and the additional noise sources which arise remove most acoustic benefits for the applications studied here. It was found that often the additional high frequencies produced inside the ejector were not not mitigated, and often were amplified, and could result in a higher EPNL than the baseline jet. And most importantly, the ejector flows were intrinsically unstable, with many configurations developing a howl for at least some flow conditions of interest. This is important to note as RANS simulations of the nozzle flows cannot predict this behavior and designs which seem promising using the traditional understanding of mixer-ejector acoustics are often very loud.

Experimental findings in this study were obtained with simplistic geometries for a given primary nozzle and with ejectors having blunt trailing edges; the method used for attaching the chevrons was also crude and left an internal step at the lip of the nozzle. However, the basic findings are considered reliable as the phenomena discussed here do not depend on these features. A list of recommendations was generated, based on the findings of this report. These recommendations start with a short list of tasks to address the assumptions that were made in the study and to validate the acoustic prediction tool *mSrc* by validating its most significant findings. The list continues with longer-term research tasks, such as recommendations to validate Large Eddy Simulation methods, both to assure they find the catastrophic resonances that RANS computations cannot detect, and to find their proper use in predicting far-field noise. Because shielding surfaces play a critical role in the mixer-ejector concept, it is recommended that acoustic liners suitable for hot, high speed flow environments be explored. Finally, it is recommended that, if the acoustic tools are found to work reliably, they be put to work by a multi-disciplinary team to design a demonstration multi-mode installed exhaust system that addresses cruise performance and LTO noise goals.

Perhaps most important for future design work, CFD and computational acoustic tools were demonstrated that relate the turbulence generated within the ejector and in the external shear layer to noise sources. This also shows the need to create optimization tools that can relate design parameters of the mixers to the turbulence, completing the relationship between nozzle geometry and noise.

Acknowledgements

The authors worked with a number of NASA researchers in various related studies during the preparation of this work. Ray Castner, Jon Seidel, Zohar Hoter, Amy Fagan, and Will Banks worked various aspects and contributed greatly to the final understanding of this topic. The authors also appreciate the helpful criticisms of our internal reviewers Cliff Brown and Vance Dippold.

Appendix A. Nomenclature and values used in study

Primary nozzle width	w	Same as ejector width	5.34 inch
Primary Nozzle height	h	Height of baseline nozzle; = A_{prim}/w all others	0.667 inch
Primary Nozzle aspect ratio	w/h	Rectangular baseline primary nozzle	8:1
Primary nozzle area	$A_{prim} = w \bullet h$	Area of mixer exit	3.562 inch^2

Ejector exit area	A_{exit}	Area of ejector exit	variable
Ejector area ratio	$EjAR = A_{exit}/A_{prim}$		variable
Ejector Inlet height Ejector Exit height	G H		variable
Ejector Length	L	Primary exit to ejector exit	variable
Ejector linear ratios	L/h	Ejector length/primary nozzle exit height	variable
Ejector Divergence Angle	α	Divergence angle set by G, H, and L.	variable
Chevron (aka tabs) parameters	Number Length Width Pattern width Penetration angle	Assumes chevrons are symmetric, repeating, flat triangles.	variable
Flow conditions	$NPR=P_{prim\_tot}/P_{\infty}$ $NTR=T_{prim\_tot}/T_{\infty}$ V_{∞}	$V_{\infty} = 0$ is CW17 condition. Note that $W_{prim} > W_{\_NPR}$ because ejector lowers pressure outside primary nozzle.	Most cases NPR=2.0, NTR=1.

IX.References

[1] Hendricks, E. and Seidel, J., 2012, "A Multidisciplinary Approach to Mixer-Ejector Analysis and Design". In *48th AIAA/ASME/SAE/ASEE Joint Propulsion Conference & Exhibit* (AIAA 2012- 4224), 2012.

[2] Huang, K.P. and Kisielowski, E., "An investigation of the thrust augmentation characteristics of jet ejectors", *USAAVLABS Report 67-8*, Contract DA-44-177-AMC-322(T), U.S. Army Aviation Materiel Laboratories, Fort Eustis, Virginia, April 1967.

[3] Quinn, B., "Compact ejector thrust augmentation", J. Aircraft, vol 10, no. 8, August, 1973.

[4] Bevilaqua, P.N., "Evaluation of hypermixing for thrust augmenting ejectors", *J. Aircraft*, vol. 11, no. 6, p. 348-354, 1974.

[5] O'Donnell, R.M. and Squyers, R.A., "V/STOL ejector short diffuser study final report", *ATC Report No. B-94300/6CR-26*, Prepared for Naval Air Development Center, Warminster, PA, June, 1976.

[6] Porter, J.L., Squayers, R.A. and Nagaraja, K.S., "An overview of ejector theory", *AIAA Paper 81-1678*, AIAA Aircraft systems and technology conference, Dayton, OH, August 11-13, 1981.

[7] Bernal, L.P. and Sarohia, V., "Entrainment and mixing in thrust augmenting ejectors", *AIAA Paper 83-0172*, 21st Aerospace Sciences Meeting, Reno, NV, Jan. 10-13, 1983.

[8] Papamoschou, D., "Analysis of partially mixed supersonic ejector", *J. Prop. & Power*, vol. 12, no. 4, p. 736-741, 1996.

[9] Heiser, W.H., "Ejector thrust augmentation", *J. Prop. & Power*, vol. 26, no. 6, p. 1325-1329, 2010.

[10] Nagaraja, K.S., "Advances in ejector technology – a tribute to Hans von Ohain's vision", *In AFWAL A collection of papers in the Aerospace Sci.*, p. 499-517, NTIS HC A99/MF A01 CSCL 20D, June 1982.

[11] Throndson, L.W., "Compound ejector thrust augmentor development", *ASME Paper 73-GT-67*, ASME Gas Turbine Conf., Washington D.C., April 8-12, 1973.

[12] Presz, W.M. Jr., Morin, B.L. and Gousy, R.G., "Forced mixer lobes in ejector designs", *J. Propulsion*, vol. 4, no. 4, p. 350-355, 1988.

[13] Presz, W.M. Jr., Reynolds, G. and McCormick, D., "Thrust augmentation using mixer-ejector-diffuser systems", *AIAA Paper 94-0020*, 32nd Aerospace Sciences Meeting, Reno, NV, January 10-13, 1994.

[14] Presz, W.M. Jr., Blinn, R.F. and Morin, B.L., "Short efficient ejector systems", *AIAA Paper 87-1837*, 23rd Joint Propulsion Conference, San Diego, CA, June 29- July 2, 1987.

[15] Long, M.J., "Experimental investigation of an ejector-powered free-jet facility", *AIAA Paper 92-3569*, 28th Joint Propulsion Conf., Nashville, TN, July 6-8, 1992. (Also NASA TM 105868).

[16] Coles, W.D., Mihaloew, J.A. and Callaghan E.E., "Turbojet engine noise reduction with mixing nozzle-ejector combinations", *NACA TN 4317*, August, 1958.

[17] Seiner, J.M. and Krejsa, E.A., "Supersonic jet noise and High Speed Civil Transport", *AIAA paper 89-2358*, 25th Joint Propulsion Conference, Monterey, CA, July 10-12, 1989.

[18] Lord, W.K., Jones, C.W., Stern A.M., Head, V.L. and Krejsa, E.A., "Mixer ejector nozzle for jet noise suppression", *AIAA Paper 90-1909*, 26th Joint Propulsion Conference, Orlando, FL, July 16-18, 1990.
[19] Presz, W.M. Jr., "Mixer/ejector noise suppressors", *AIAA Paper 91-2243*, 27th Joint Propulsion Conference, Sacramento, CA, June 24-26, 1991.
[20] DeBonis, J.R., "Full Navier-Stokes analysis of a two-dimensional mixer/ejector nozzle for noise suppression", *AIAA Paper 92-3570*, 28th Joint Propulsion Conference, Nashville, TN, July 6-8, 1992.
[21] Tillman, T.G. and Presz, W.M. Jr., "Thrust characteristics of a supersonic mixer ejector", *J. Prop. & Power*, vol. 11, no. 5, p. 931-937, 1995.
[22] Majjigi, R.K., Balan, C., Mengle, V., Brausch, J.F., Shin, H. and Askew, J.W., "Low noise exhaust nozzle technology development", *NASA CR 2005-213325*, February, 2005 (originally published as NASA Report HSR044, Nov., 1996).
[23] Dickson, N., "ICAO Noise standards", International Civil Aviation Organization Symposium on aviation and climate change, Montreal, Canada, May 14-16, 2013.
[24] Henderson, B.S., Bridges, J., Wernet, M.P., "Jet Noise Reduction Potential from Emerging Variable Cycle Technologies", AIAA 2012-3752, AIAA/ASME/SAE/ASEE Joint Propulsion Conference, Atlanta, 2012.
[25] Hoter, Z., Castner, T.S., Zaman, K.Q., "CFD Optimization of Ejector Flaps in a One-Sided Ejector" ,AIAA 2019-0544, AIAA SciTech 2019 Forum, San Diego, 2019.
[26] Zaman, K.Q., Fagan, A.F. and Bridges, J., "Experimental investigation of a one-sided ejector nozzle", In *AIAA Scitech 2019 Forum* (AIAA 2019-0543), 2019.
[27] Zaman, K.Q., Bridges, J., Castner, R.S. and Fagan, A.F., "An investigation of a mixer-ejector nozzle for jet noise reduction". In *25th AIAA/CEAS Aeroacoustics Conference* (AIAA 2019-2494), 2019.
[28] Zaman, K.Q., Castner, R.S., Bridges, J., Fagan, A.F. and Upadhyay, P., "Experiments on Thrust, Flowfield and Noise of a Rectangular Mixer-Ejector Nozzle". In *AIAA Scitech 2020 Forum* (AIAA 2020-0003), 2020.
[29] Burt, J.M., Seidel, J. and Leib, S.J., "Assessment of Mixer-Ejector Nozzle with Thermal Acoustic Shield for Jet Noise Reduction". In *AIAA Aviation 2019 Forum* (AIAA 2019-3018) 2019.
[30] Bridges, J.E., "Noise measurements of a low-noise top-mounted propulsion installation for a supersonic airliner". In *AIAA Scitech 2019 Forum* (AIAA 2019-0253) 2019.
[31] McDonald, T.J. and Estenson, A.S., "Cold-Flow Model Tests to Determine Static Performance of a NASA One-Sided Ejector Nozzle System," NASA/CR-2020-220453, (2020).
[32] Fisher, M.J., Lush, P.A. and Harper Bourne, M., "Jet noise," *Journal of Sound Vibration*, *28*, pp.563-585 (1973).
[33] Bridges, J., "Rapid Prediction of Installed Jet Noise From RANS", *AIAA paper 2020-2732*, AIAA/CEAS Aeroacoustics Conference, The Netherlands, 2019.
[34] Bridges, J. and Brown, C., " Validation of the small hot jet acoustic rig for aeroacoustic research," In *11th AIAA/CEAS Aeroacoustics Conference* (AIAA 2020-2846), 2005.
[35] Morgenstern, John, Michael Buonanno, Jixian Yao, Mugam Murugappan, Umesh Paliath, Lawrence Cheung, Ivan Malcevic et al. "Advanced concept studies for supersonic commercial transports entering service in the 2018-2020 period phase 2." 2015.